In-situ single step synthesis of $MoSi_2$ nano powder

A

Thesis

Submitted in partial fulfillment of the

requirements for the award of degree of

MASTER OF SCIENCE

by

Taranpreet Kaur

(Registration No. 301504036)

Under the Supervision of

Dr. O.P. Pandey

(Senior Professor)

School of Physics & Materials Science

Thapar University, Patiala-147004

July, 2017

CERTIFICATE

This is to certify that this dissertation entitled **'In-situ single step synthesis of $MoSi_2$ nano powder'** is submitted by **Ms. Taranpreet Kaur** (Registration No. 301504036) in the fulfillment of the requirement for the award of degree of Master of Science in Physics from School of Physics and Materials Science, Thapar University, Patiala (Punjab), India. It is an exclusive record of candidate's own research under the supervision of **Dr. Om Prakash Pandey**. This dissertation in part or full has not been submitted in any other institution for the award of such kind of degree.

Dr. Om Prakash Pandey

(Supervisor)

Senior Professor and Dean (R&SP)

School of Physics and Materials Science

Thapar University, Patiala

ACKNOWLEDGEMENT

I am submitting my dissertation for the fulfillment of my 'M.Sc.' degree in Physics. This work would not have been accomplished without the support, help and guidance of a large number of people. I express my deep gratitude and respect to my supervisor **Dr. O.P. Pandey,** Senior Professor and Dean (R&SP) for his keen interest, strong motivation and constant encouragement during the course of the work. I thank him for his great patience, constructive criticism and myriad useful suggestions apart from invaluable guidance to me.

I would also like to thank **Dr. Manoj Sharma** (Head of Department) and all other faculty members of School of Physics and Materials Science for their constructive suggestions at different stages of this work.

I would like to thank to **Mr. Piyush Sharma, Mr. Aayush Gupta and Mr. Mir Rameez** for their moral support and constant co-operation whenever required.

I am also thankful of my friends Ms. Ruby Priya, Ms. Rupinderjeet, Ms. Rajpal kaur, Ms. Harneet Kaur, Mr. Amit Singh and Mr. Varun Singhal for their support during my project work.

The meaning of my life and work is incomplete without paying regards to my respected family whose blessings and continuous encouragement have shown me the path to achieve my goals.

And above all, I pay my regards to the Almighty for his blessings.

Taranpreet Kaur

Taranpreet Kaur

ABSTRACT

Molybdenum disilicide ($MoSi_2$) has emerged as a promising material for high temperature applications. This transition metal silicide exhibits superior temperature stability, excellent oxidation resistance, low contact resistivity and is highly resistant to electro-migration. The low temperature synthesis of molybdenum disilicide has been investigated in a specially designed autoclave. The powder blend of MoO_3-Si-Mg is heated at different temperatures for various interval of time. The impact of initial composition of the formation of $MoSi_2$ is also studied. The prepared samples are characterized through various techniques i.e. X- ray diffraction (XRD), Field emission scanning electron microscope (FE-SEM) and high-resolution transmission electron microscope (HRTEM). The best results are obtained at 900 ºC for 10 hrs. dwell time. In this case, molybdenum disilicide ($MoSi_2$) phase is obtained along with molybdenum silicide (Mo_5Si_3). This study provides the complete understanding associated with the formation of $MoSi_2$.

LIST OF FIGURES

LIST OF TABLES

CHAPTER 1: INTRODUCTION

CHAPTER 3: EXPERIMENTAL DETAILS

TABLE OF CONTENTS

1.1. Introduction

Nowadays, modern technology is totally dependent on microelectronic devices. The ongoing progress in the field of microelectronics brings a new technological revolution which have significantly transformed the shape of modern society. The novel microelectronic devices possess high processing speed, excellent flexibility, low cost and consume less energy. The wider applicability of these devices led to significant enhancement in productivity in industries, agriculture, office management, education, health and communications **[1]**. The microelectronic devices essentially require very large-scale integration (VLSI) of several components such as transistors, resistors and capacitors, on a silicon chip **[2]**. Also, the performance of these devices significantly depends on the quality of integration accomplished through interconnecting wire or interconnects of metallic conductors. In order to enhance performance of these devices, interconnecting material must possess high electrical conductivity, low contact resistivity and good junction interface are essentially required **[3].**

In the current scenario, transition metal silicides emerge as a suitable candidate for contact material in electronic industries. Transition metal silicides possess low contact resistivity and outstanding junction interface with silicon **[4].** In addition, these materials offer unique range of electronic, magnetic, optical, catalytic, and mechanical properties. Rapid growth of transition metal silicides with diversified properties have attracted interest for nanoscale devices. Transition metal silicides as a good contact material serve crucial role in nanoelectronics and photonics technology. These compounds can be significantly used in variety of technological application such as complementary metal-oxide-semiconductor (CMOS) devices, thin-film coatings, nanoelectronics, field emitter's electrical heating elements, spintronics, photovoltaics, thermoelectric and many more **[5].**

1.2. Transition metal silicides

Basically, transition metal silicides are recognized as an important family of inorganic materials that exhibit superior properties. These materials are intermetallic compounds of transition metals and silicon. Among all transition metal silicides, only silicides of groups IVA, VA, VIA and VIII are of special interest. The metal silicides of groups IVA, VA and VIA are known as refractory metal silicides and of group VIII are termed as near-noble-metal silicides. The refractory transition metal silicides have high melting points and can be used in high temperature

applications **[2]**. On the other side, near noble transition metal silicides can be employed in low temperature applications. Generally, transition metal silicides with high silicon content are more stable and conducting. The properties of metal silicide significantly depend upon the parent metals, stoichiometries, synthesis route and crystal structures. Transition metal silicides exhibit unique electronic and crystal structures as compared to their parent metals due to the strong interaction of transition metals with silicon **[6]**.

The continuous trend of device miniaturization seeks the scientist's attention toward nanostructured metal silicide. These materials provide attractive choice for nanoscale field emitters and biological applications **[7]**. The emergent demand of metal silicides is due to their low resistivity like metals and high temperature stability. Metal silicides are highly resistant to electro-migration, which makes them promising materials for gate and interconnection metallization. These compounds have potential to encounter the needs of modern technological applications, at nanoscale. Out of all refractory silicides, molybdenum silicide emerges as a potential candidate for a new mission focusing at elevated temperature suitability of novel electronic devices **[8]**.

1.3. Molybdenum Silicide

Molybdenum silicide exist in three different forms depending upon the silicon content i.e. mono-silicide (Mo_3Si), disilicide ($MoSi_2$) and 5-3 silicides (Mo_5Si_3), as shown in figure 1.1 **[8]**. Among these molybdenum silicides, silicon rich disilicides are widely used at elevated temperature because it offers high corrosion resistance. In addition, $MoSi_2$ exhibit excellent oxidation resistance even at higher temperature due to the formation of protective silica layer (SiO_2) during heat treatment **[9]**.

1.4. Binary Phase diagram of Mo-Si system

Binary phase diagram plays a crucial role in understanding the formation of distinct phases of two components system at different temperature and composition. This leads to the identification of appropriate condition required for the formation of a particular phase. In order to understand the formation of different phases of Mo-Si system, the equilibrium diagram is presented in Fig. 1.2. Also, various intermediate phases formed with the variation of Si content and temperature are tabulated in table 1.1.

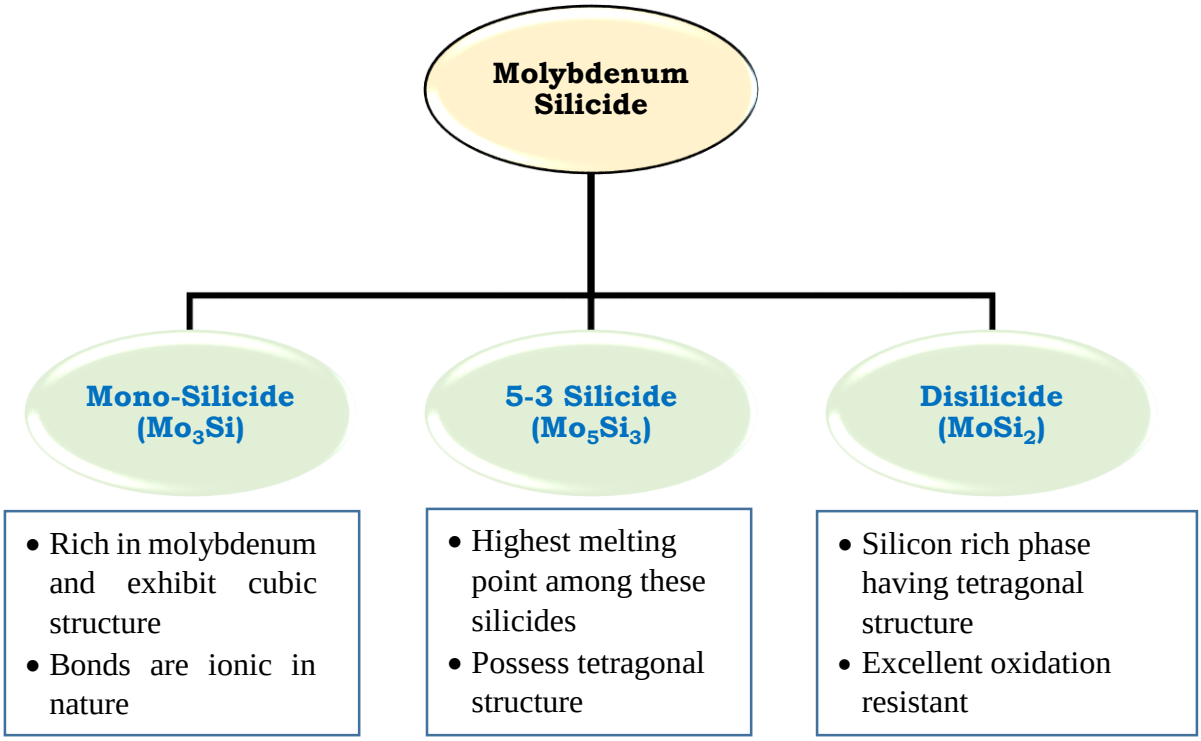

Fig. 1.1 Three different forms of molybdenum silicide.

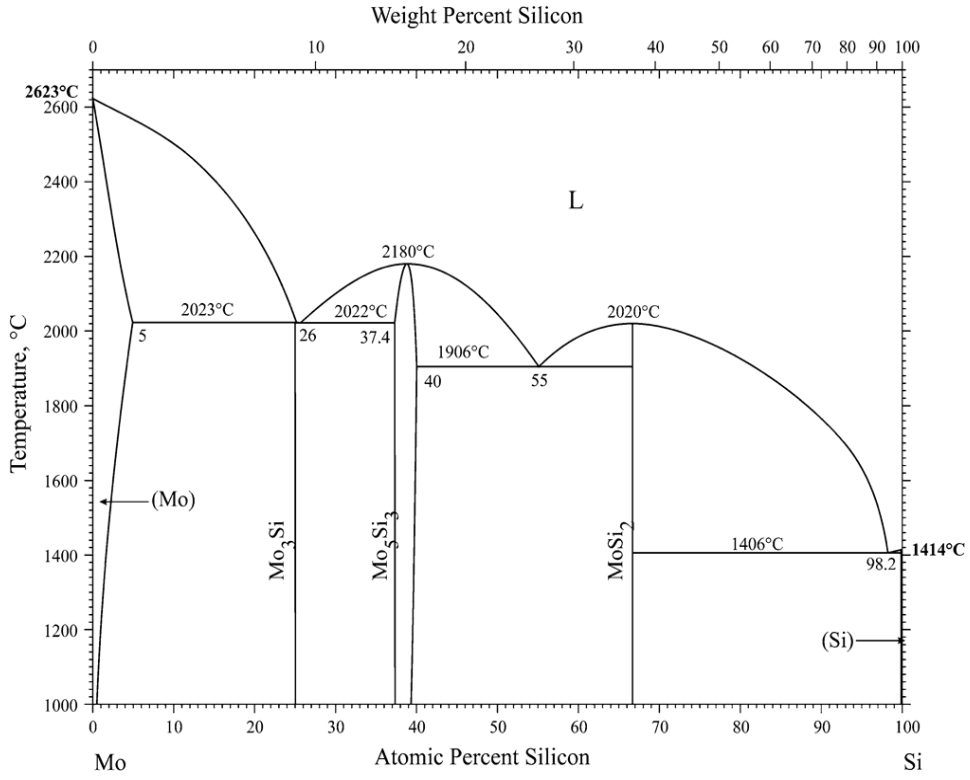

Fig. 1.2 Binary phase diagram of Mo-Si system **[10]**.

Table 1.1: Various intermediate phases of Mo-Si system formed by varying Si content and temperature.

Si content (at. %)	Temperature (˚C)	Phases
0	2623	Mo melting
5-26	2023	Mo_3Si
26-37.4	2022	Mo_5Si_3
37.4	2180	Mo_5Si_3 melt congruently
40-66.7	1906	β-$MoSi_2$
66.7	2020	β-$MoSi_2$ melt congruently
66.7	1906	α-$MoSi_2$
66.7-98.2	1406	Si
100	1414	Si melting

In Mo-Si system, three intermediate phases exist such as Mo_3Si, Mo_5Si_3 and $MoSi_2$. The upper portion of phase diagram (Fig. 1.2) shows liquid phase (L) of Mo-Si system. The phase diagram shows that the maximum solubility of silicon is up to 4 at% in molybdenum at 2023 ˚C. Further increase in silicon content (up to 26 at%) results into formation of molybdenum rich compound i.e. Mo_3Si at 2023˚C. This phase transforms to Mo_5Si_3 when the silicon content is 26 at %. Afterwards, Mo_5Si_3 phase melt congruently at 2180˚C with 37.6 at% silicon and it starts to transform into molybdenum disilicide (α-$MoSi_2$) at 1906˚C.

The complete transformation of Mo_5Si_3 phase to α-$MoSi_2$ occurs, when the silicon content is increased to 66.7 at%. It is also clearly visible from the phase diagram that α-$MoSi_2$ transforms to β-$MoSi_2$, at 1906˚C. This intermediate phase of Mo-Si system (β-$MoSi_2$) starts to melt congruently at 2020˚C. At 1406˚C, as the silicon content is increased to 98.2 at%, pure silicon phase is observed. This silicon phase starts to melt at 1414˚C exhibiting 100 at% silicon. Thus, binary phase diagram represents the formation of molybdenum disilicide ($MoSi_2$) at 1906˚C with 66.7 at% Si. Among all these intermediate phases, molybdenum disilicide ($MoSi_2$) possess high oxidation resistance at elevated temperature as compared to other phases. In this phase, a protective layer SiO_2 forms at higher temperatures. This phase of Mo-Si system is extensively used as heating element **[10]**.

1.5. Molybdenum Disilicide

Molybdenum disilicide is an intermetallic compound which consists of metallic and covalent bonding. It is used as higher temperature structural material as it possesses a unique combination of properties such as high melting point (2030ºC), moderate density (6.24 g/cm^{-3}), high temperature strength, excellent resistance to oxidation, high electrical and thermal conductivity. Molybdenum disilicide possess polymorphic nature and exhibit two phases i.e. tetragonal phase (α-$MoSi_2$, C11 type) and hexagonal phase (β-$MoSi_2$, C40 type) [6]. Above 1900ºC, tetragonal phase transforms to hexagonal phase. This behavior leads to differentiate it from high temperature materials such as ceramic and intermetallic **[11].** Based on these wider properties, $MoSi_2$ is extensively used as furnace heating element and high temperature corrosion-protective material. It also emerges as an attractive wear-resistant material for room and high temperature corrosive and oxidative environments. In addition, molybdenum disilicide thin film coating plays a crucial role as contacts and interconnects in microelectronic industries **[12]**.

1.6. Crystal structure of molybdenum disilicide

Molybdenum disilicides exhibit tetragonal unit cell structure consists of stacking three body centered cube along the direction of 'c' in which one molybdenum (Mo) layer is followed by two silicon (Si) layer. Figure 1.3 shows the crystal structure of molybdenum disilicides. The body centered tetragonal structure stacked one on top of another in which body- centered site is occupied by atom of Mo or Si alternately **[13]**.

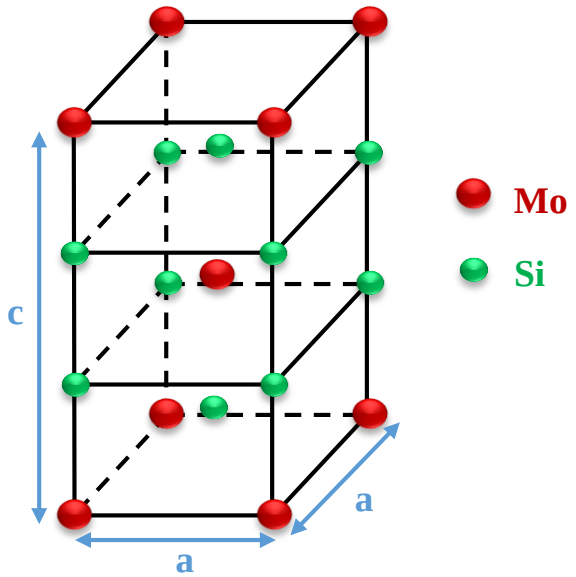

Fig. 1.3 Crystal structure of molybdenum disilicide ($MoSi_2$).

1.7. Synthesis routes

1.7.1. Solid state reaction

The most widely used method for preparation of polycrystalline solids is solid state reaction (SSR) **[14]**. In this method, polycrystalline solids are prepared from mixture of solid starting materials. Since, in this technique solid do not react with each other at room temperature (RT), so it is necessary that solids are heated at elevated temperature for the proper reaction to take place at appreciable rate. The final product of SSR is mostly in the form of a powder or a sintered, polycrystalline piece.

1.7.2. Spark plasma sintering

Sintering is a process in which material is heated in furnace below its melting point such that by diffusion of atoms, bonding takes place and hence, objects are formed from powder by this process. Spark plasma sintering involves the consolidation of the powder by using uniaxial force and a pulsed direct electrical current under low atmospheric pressure **[15]**.

1.7.3. Chemical vapor deposition (CVD)

It is the technique in which the wafer (substrate) is exposed to one or more volatile (gaseous reactants) precursors and further reacts or decompose on the substrate surface in order to produce desired deposit **[14]**. The final material obtained through this method is of good quality, high purity and exhibit excellent performance. This method is extensively used in wide range of applications such as in semiconductor industry to produce thin films, integrated circuits and in other micro-devices.

1.7.4. Chemical vapor transport (CVT)

In chemical vapor transport method, interaction between solid and a volatile compound occurs due to which a solid product is deposited **[14]**. This implies that this method involves thermodynamic reaction between two chemical species such as source material and a transport agent, in order to produce gas-phase precursors in situ. The elements required to synthesize the desired phase are provided by intermediates. Single crystals of metal silicides are synthesized by this technique, usually, at high temperature.

1.7.5. Mechano-chemical Synthesis

It involves repeated welding, deformation and fracture of the reactants mixture and during milling process, chemical reactions are re-generated continuously at the interface of nanometer-

sized grains as a result chemical reaction occurs at the low temperature in the ball mill **[16]**. Therefore, mechano-chemical processing is used to synthesize nano-crystalline particles under suitable conditions such as chemical reaction path, stoichiometry of starting material and milling condition.

1.7.6. Self-propagating high temperature synthesis

The process in which, initial reagents immediately ignites to form product by exothermic reaction is called self-propagating high temperature synthesis **[17]**. The combustion synthesis, gasless combustion, self-propagating combustion, self- propagating exothermic reaction represents the same process (SHS).

1.8. Applications

Molybdenum disilicide exhibits wide range of properties such as good electrical conductivity, excellent oxidation resistance, high strength and modulus of elasticity at higher temperature. These wide range of properties suggest that molybdenum disilicide is highly suitable for different industrial applications. The applicability of $MoSi_2$ at elevated temperature makes it potential candidate for heating element, aerospace gas turbine engine, industrial gas burner, diesel engine glow plugs, glass processing and corrosion protective coating **[13]**. The brief description of all these applications are as follows:

1.8.1. Heating element

The heating element of molybdenum disilicide is extensively used in industrial furnaces for sintering, glass melting and heat treatment forging and in laboratory furnaces. Molybdenum disilicide has a capability of forming a protective layer of quartz (SiO_2) after reacting with oxygen at elevated temperatures. Also, lower silicon molybdenum silicide (Mo_5Si_3) is formed under the SiO_2 layer **[13]**. The heating element made of $MoSi_2$ can be operated upto 1900 ºC.

1.8.2. Gas turbine engines

In gas turbine engines, the outer seal of blades is a stationary part, which is located just opposite to the rotating hot section turbine blades **[18]**. The purpose of this outer seal is to maintain a small gap of stable dimensions with the turbine blade. Therefore, material used for this purpose is made of molybdenum disilicide because it helps in enhancing the efficiency of turbine blades by reducing thermal stress in ultra- high temperature combustion system.

1.8.3. Industrial gas burners

In the current era, the gas burner industry focusing on the development of burners made of oxygen-natural gas mixtures rather than air-natural gas mixtures **[19]**. This will lead to reduction in environmental NO_x emissions. Moreover, these burners should be operated at higher temperature. So, $MoSi_2$ emerge as a suitable candidate for these gas burners due to its good oxidation resistance at higher temperature.

1.8.4. Diesel engines

In a diesel engine, glow plug plays crucial role as a primarily heating device for starting up the engine **[18]**. These glow plugs comprise of inner composite cylinder made of molybdenum disilicide ($MoSi_2$). This increases life time of glow plugs and also highly resistant to diesel fuel combustion environment. Moreover, glow plugs made of molybdenum disilicide ($MoSi_2$) can be heated at higher heating rate for the engine to be started faster.

1.8.5. Glass processing

Presently, metals and ceramic refractories are extensively used for the development of new components which essentially require contact with molten glasses **[20]**. In this application, $MoSi_2$ is widely used because it offers high resistance to corrosion and exhibit excellent oxidation resistance above the glass line due to the formation silicon oxide (SiO_2) layer.

References

[1] Wad, *Microelectronics: implications and strategies of the third world* 4 (1982) 677-697, Taylors & Francis. Ltd.

[2] S.P. Muraka, *Transition metal Silicides*, Annual Review of material Science 13 (1983) 117-137.

[3] L.J. Chen, Silicide technology for Integrated circuits - *Silicides an introduction*, The institute of Electrical Engineers, London, U.K (2004).

[4] Y.C. Lin, Y. Chen and Y. Huang, *The growth and applications of silicides for nanoscale devices*, Nanoscale 4 (2012) 1412-1421.

[5] A.L. Schmitt, Jeremy, M. Higgins and S. Jin, *synthesis and applications of metal silicide nanowires*, Journals of material chemistry 20 (2010) 223-235.

[6] X. Chen, J.C. Guan, G. Sha, Z. Gao and C. Liang, *preparation and magnetic properties of single phase Ni_2Si by reverse Rochow reaction*, RSC Advances 4 (2014) 653-659.

[7] J.Y Lin, H.M Hsu and K.C Lu, *Growth of single -crystalline nickel silicide nanowires with excellent physical properties*, Crystal Engineering Communication 17 (2015) 1911-1916.

[8] R.A. Mackay, S.D. Antolovich, R.W. Stusrud, D.L. Anton, T. Khan, R.D. Kissinger, D.L. Klarstrom, Superalloys - *$MoSi_2$ and other silicides as high temperature structural materials*, The Minerals, Metals & Materials Society, (1992).

[9] D. Ovali, D. Agaogullan, *Effects of excess reactant amounts on the mechano-chemically synthesized molybdenum silicides from MoO_3, SiO_2 and Mg Blends,* International Journal of Refractory and Hard materials 65 (2016)19-24.

[10] A.B. Gokhale, G.J. Abbaschian, *The Mo- Si (Molybdenum –Silicon) system,* Journal of Phase Equilibria 12 (1991) 493-498.

[11] R.B. Schwarz, S.R. Srinivasan, J.J. Petrovic, *Synthesis of molybdenum disilicide by mechanical alloying,* Materials Science and Engineering A155 (1992) 75-83.

[12] Z. Yao, J. Stiglich and T.S Sudarshan, *Molybdenum silicide based materials and their properties, Journal* of materials Engineering and Performance (1999) 291-304.

[13] S.P. Mauraka, *Refractory silicides for integrated circuits,* Journal of Vacuum Science and Technology 17(1980) 775-791.

[14] J.M. Higgins, A.L. Schmitt and S. Jin, *Synthesis and applications of metal silicide nanowires,* Journal of Materials Chemistry 20 (2010) 223-235.

[15] B. Ertug, Sintering Applications - *Challenges and opportunities for spark plasma sintering: A key technology for a new generation of materials*, InTech (2013).

[16] T. Tsuzuki, P.G. McCormick, *Mechano-chemical synthesis of nanoparticles*, Journal of Materials Science 39 (2004) 5143-5146.

[17] J. Subrahmanyam, M. Vijayakumar, *Self-propagating high – temperature synthesis*, Journal of Materials Science 27 (1992) 6249-6273.

[18] J.J. Petrovic, *High Temperature Structural Silicides*, Ceram Engineering and Science Proceedings 18 (1997) 3-17.

[19] W.Y. Lin, J.Y. Hsu, R.F. Speyer, *Stability of Molybdenum Disilicide in Combustion Gas Environments*, Journal of the American Ceramic Society 77 (1994) 1162-1168.

[20] S.K. Sundaram, R.F. Speyer, *Electrochemical Corrosion and Protection of Molybdenum and Molybdenum Disilicide in a Molten Soda-Lime Silicate Glass Environment*, Journal of the American Ceramic Society 79 (1996) 1851-1856.

2.1. LITERATURE REVIEW

Molybdenum disilicide ($MoSi_2$) has attained significant attention from various researchers. $MoSi_2$ can be employed in plethora of application such as CMOS devices, thin-film coatings, nanoelectronics, field emitters electrical heating elements, spintronics, photovoltaics and many more. Still there are several research groups involved to investigate appropriate synthesis route and superior properties of $MoSi_2$.

In 1991, Zhang *et al.* [**1]** synthesized molybdenum disilicide by self-propagating combustion method. They prepared three phases of molybdenum silicides (Mo_3Si, Mo_5Si_3 and $MoSi_2$); among them first two phases required preheating for the ignition of self-sustaining mode. The last phase ($MoSi_2$) can be prepared without pre-heating the starting reactants. The X-ray analysis revealed that the products of the combustion between Mo+2Si mixture was multiphase for Si less than 37 wt%. However, $MoSi_2$ along with small amount of Si was obtained when the silicon content was greater than 37 wt%. Schwarz *et al.* [**2]** used high energy-ball-milling process and synthesized alloy powders of $MoSi_2$, $MoSi_2$-27 mol% Mo_5Si_3 and $MoSi_2$-50 mol% Mo_5Si_3 from elemental powders (Mo and Si). The milled powders were hot-pressed at 1500 ºC and 12MPa pressure. The compacts achieved from the mechanically alloyed powder showed higher density ($7.09 g/cm^{-3}$).

The formation mechanism involved during mechanical alloying of molybdenum disilicide was investigated by Yen *et al.* [**3**]. The result revealed that the reaction rate and formation of $MoSi_2$ during mechanical alloying depends on the powder composition. They observed that the variation in the silicon content affect the final stoichiometric of the product. When the Si content was 67 at%; the α-$MoSi_2$ was formed. However, with the excess amount of Mo and Si, powdered mixture showed the formation of α-$MoSi_2$ and β-$MoSi_2$. Further, the mechanical properties of monolithic molybdenum disilicide prepared by spark plasma sintering (SPS) was studied by Shimizu *et al.* [**4**]. It was observed that dense molybdenum disilicide fabricated at 1300ºC possess excellent mechanical properties. X-ray diffraction (XRD) pattern showed that powder includes $MoSi_2$ and small amount of Mo_5Si_3. The powder sintered at 1300ºC, contains two phases $MoSi_2$ and SiO_2. As sintering temperature increased, grain size of molybdenum disilicide increased slowly at 1400ºC and change abruptly between 1400º C- 1500º C. Moreover, at 1400º C-1500º C, monolithic $MoSi_2$

materials possess high strength as compared to conventional $MoSi_2$. The powder sintered at 1300ºC showed superior properties than sintered at 1200ºC and ≥ 1400ºC.

The effect of aluminosilicate on the microstructure and low temperature oxidation of $MoSi_2$ was reported by Wang *et al.* [**5]**. It was observed that the additive oxide (aluminosilicate) ≤ 15 vol% was uniformly dispersed in the $MoSi_2$ matrix. As the oxide content increased, the network of microstructure was formed after the intermixing of both constituent phase. The further increased in oxide content (upto 45 vol%), the distribution of $MoSi_2$ changed from continuous phase to isolated phase. The above observation concluded that, the composites were easily oxidized. Moreover, the grain boundary affects the low temperature oxidation. The 10 vol% additive oxides located at point boundaries and edge point of $MoSi_2$ possess oxidation but more than 50 vol% oxides at edge boundary of $MoSi_2$ blocked the path for oxygen diffusion.

Jianguang *et al.* [**6**] prepared the pure molybdenum disilicide by chemical-oven self-propagating combustion method (COSHS) and self-propagating combustion method (SHS). The products obtained from both methods (COSHS and SHS) showed $MoSi_2$ with few traces of Si and Mo_5Si_3 without the addition of ammonium chloride (NH_4Cl). However, pure $MoSi_2$ was formed through COSHS by adding 4 wt% NH_4Cl. It was observed that pure $MoSi_2$ exhibit more homogeneous and less agglomerated particles, as evident from scanning electron microscopy (SEM).

Kuchino *et al.* [**7]** performed sintering of commercially available $MoSi_2$ and mixture of Mo+2Si through spark plasma sintering (SPS). They observed that SiO_2 inclusions were formed in both sintered samples but the formation of SiO_2 inclusions in-situ synthesis (Mo and Si mixture) was lowered than that of commercially $MoSi_2$ powder. Further, transmission electron microscopy (TEM) revealed that SiO_2 inclusions were formed at grain boundaries of $MoSi_2$ whereas no inclusions of SiO_2 were observed in- situ synthesis.

The microalloying of molybdenum disilicide by two activation processes (mechanical activation and field activation) was performed by Woolman *et al.* [**8]**. The results of X-ray diffraction revealed that α-$MoSi_2$, β-$MoSi_2$ and unreacted Mo phases were observed after 10 hrs milling of powder sample. As the milling time was increased to 24 hrs, the α-$MoSi_2$ was found to be absent in the sample. In the case of field activation process, the SPS sintered un-milled powder samples exhibit Mg, α-$MoSi_2$, Mo_5Si_3 and unreacted Mo phases. However, no Mg peak in XRD

was observed after SPS of milled sample. They concluded that the ductile-brittle transition temperature was reduced with the addition of Mg.

Zakeri *et al.* [**9**] synthesized nano-crystalline $MoSi_2$ by mechanical alloying. They observed broadening in the peaks of Mo and sharp decrease in the intensity of Si peaks as the milling time was increased from 0-20hrs. They concluded that Si peaks disappeared and α-$MoSi_2$ peaks appeared with increased in milling time (30hrs, 50hrs and 70hrs) of sample. They also observed the effect of heat treatment on $MoSi_2$ phase by annealing two mechanically alloyed sample (10hrs and 30hrs). At 600ºC, Mo and Si peaks were observed in 10hrs milled sample. As temperature was increased 1000ºC; a trace amount of α-$MoSi_2$ was formed. In the case of 30hrs milled sample, only Mo peaks were observed at 600ºC. However, further increase in temperature (1000ºC) resulted into formation of $MoSi_2$.

Moreover, the effect of pest oxidation on single crystal $MoSi_2$ and spark plasma sintered poly-crystalline $MoSi_2$ at 773K was studied by Zhang *et al.* [**10]**. They observed that $MoSi_2$ (either poly or single crystalline) exhibited micro-cracks resulting into pest oxidation (at 773K). Microstructure analysis showed that $MoSi_2$ phase was obtained in single crystal but polycrystalline possessed $MoSi_2$ along with minor phases such as SiO_2 and Mo_5Si_3. Further, oxidation kinetic followed was parabolic in single crystal while linear kinetics was observed in dense poly-crystalline $MoSi_2$. Surface morphologies revealed that oxide scale formed on single crystal was uniform and dense without defects and cracks whereas poly-crystal oxide scale was porous and full of micro-cracks.

Xu *et al.* [**11**] investigated the effect of vacuum and argon atmosphere on $MoSi_2$ synthesizes through self-propagating combustion method. They also investigated the processing parameters such as exothermicity, heating rate and particle size of $MoSi_2$. It was observed that higher heating rate and maximum temperature was produced in argon atmosphere during self-propagating combustion synthesis. Moreover, the average particle size of $MoSi_2$ in vacuum was more than that in argon atmosphere. Also, the particle size distribution of $MoSi_2$ was more homogeneous in argon atmosphere. X-ray diffraction results revealed that in addition to $MoSi_2$ small amount of Mo and Mo_5Si_3 were observed in argon atmosphere than that of vacuum. X- ray fluorescence analysis showed that product formed in the presence of argon was pure due to the evaporation of impurities at maximum. They concluded that in argon atmosphere low temperature

gradient resulted in higher heating rate, reaction rate and faster propagation in Self-propagating combustion synthesis.

Cabouro and his co-workers [**12]** studied the reactive sintering of molybdenum disilicide by spark plasma sintering **(**SPS) prepared from mechanically activated powder mixture of Mo and Si. It was observed that relative density of $MoSi_2$ increased when the SPS processing parameters (heating rate, applied pressure and SPS holding time) were increased to a critical value. The oxidation behavior of $MoSi_2$ was also determined at low temperature (673-873K). They showed that the formation of molybdenum oxide (MoO_3) occurred at low temperature (673K) due to the pest oxidation of $MoSi_2$. However, the growth of MoO_3 decreased in nano-organized $MoSi_2$ (ball milled) at 673K due to the presence of silica layer on its surface. Also, the formation of silica layer improved the corrosion resistance of $MoSi_2$.

In addition, the energy analysis of mechanically alloyed molybdenum disilicide was conducted by Zhong and his co-workers [**13]**. It was observed that the extent to which vial filled, showed a significant effect on efficiency factor and total energy of milling process. When the vial was half full of balls, the efficiency of mechanically alloyed process was excellent. They showed that the incubation time of mechanically alloyed self-propagating reaction (MSR) was reduced when BPR was 15:1 but in half full of balls, ball milling time was increased (90min) to attain a particular phase of powder. They observed that $MoSi_2$ can be easily obtained when the vial was two-third or one-third full. They observed that efficiency range was 1.944- 8.507 kJ/ (g.s) and total milling energy was 19.38-26.47 kJ/g for the MSR of 1Mo:2Si powder mixture.

Furthermore, the effect of variation in the content of starting material on the incubation time and phase formation through mechanically induced self-propagating reaction (MSR) was studied by Feng *et al.* [**14]**. They observed that excess amount of Mo of powder mixture (Mo and Si) raised the rate of MSR whereas Si rich powder mixture extended the incubation time. Moreover, mechanical alloying can't induce self-propagating reaction when the deviation of Mo or Si content was higher (1.0Mo:1.0Si and 1.0Mo:3.0Si) in molar ratio from $MoSi_2$ stiochiometry. They concluded that with excess amount of Mo in powder mixture, Mo_5Si_3 was formed. However, pure phase of $MoSi_2$ was obtained when MSR occurred. Nersisyan *et al.* [**15]** studied the effect of sodium chloride (NaCl) on the combustion system (MoO_3+SiO_2+Mg) to synthesize fine powder of $MoSi_2$. They observed that the combustion reaction with the addition of 5-14 mol% NaCl. The

results of reported paper, indicated that the reaction (MoO_3+9Mg+3SiO_2+αNaCl→ $MoSi_2$ +9MgO+Si+α NaCl) was most favorable for the formation of $MoSi_2$.

The effect of molybdenum (Mo) particle size on self-propagating high temperature synthesis (SHS) was investigated by Khoshkhoo *et al.* [**16**]. They observed that microstructure comprised of equiaxed $MoSi_2$ grain when the Mo particle size was small (149 microns). The reaction rate of SHS mechanism became shorter on the dissolution of smaller Mo particles in molten silicon followed by precipitation of $MoSi_2$. However, Mo_5Si_3 and Mo_3Si products were formed around the unreacted Mo particles when the size of Mo particle was large. Feng *et al.* [**17**] investigated the effect of diluent ($MoSi_2$) on the synthesis of molybdenum disilicide by (MSR). They observed that incubation period of MSR was increased by adding diluent ($MoSi_2$) from 0 wt% to 10 wt% to powder mixture of Mo and Si. Further, the extended incubation period decreased the adiabatic temperature and increased the ignition temperature of MSR. Also, the addition of diluent to Mo-Si powder mixture resulted into the formation of pure $MoSi_2$.

Cabouro *et al.* [**18]** synthesized dense $MoSi_2$ through reactive flash sintering. The agglomerates (0.8 to 800μm) of molybdenum and silicon were formed due to continuous fracture-welding process with high energy ball mill. This resulted into the increase in reactivity of mixture (Mo and Si). The XRD result showed that dense $MoSi_2$ of lower molybdenum silicide (Mo_5Si_3) content is obtained from the powder mixture without sieving. Yamada *et al.* [**19]** synthesized the β and α- $MoSi_2$ powder using Na metal at low temperature (873K and 1073K). The single phase β- $MoSi_2$ and α-$MoSi_2$ were obtained and 1073K and 973K respectively. They observed that the formation of α-$MoSi_2$ along with Mo_5Si_3 occurred at 1173K. They also prepared $MoSi_2$ through plasma spray synthesis. During this process, the mixture of α and β $MoSi_2$ were formed at 973K. They observed that thermal annealing of powder mixture (Mo and Si) above 973K showed an irreversible transformation (β-$MoSi_2$ to α-$MoSi_2$). The morphology of the sample prepared through plasma spray showed irregular and angular grains of α and β $MoSi_2$ with size < 2μm.

Hasani *et al.* [**20]** studied the effect of atmosphere and heating rate on the formation mechanism of $MoSi_2$ by exposing Mo+2Si powder mixture to simultaneous thermal analysis at different heating rate. Thermal analysis results showed that air atmosphere and low heating rate leads to surface oxidation of Mo. They observed that higher heating rate didn't affect the type of

atmosphere for $MoSi_2$. However, the final products were strongly affected by the type of atmosphere at low heating rate.

Yan *et al.* [**21**] investigated the effect of sprayed powder ($MoSi_2$) size on the phase composition, microstructure, bonding strength and micro-hardness of $MoSi_2$ coating formed by air plasma spray (APS). After coating of $MoSi_2$, the XRD results revealed the formation of α-$MoSi_2$ and β-$MoSi_2$, Mo_5Si_3, MoO_3 phases. Also, increased in spray powder size during spraying process, reduced the oxidation of $MoSi_2$. They showed that as the sprayed powder size increased, porosity increased which decreased the bonding strength of $MoSi_2$ coatings. However, the hardness of $MoSi_2$ coatings was firstly increased and then decreased with increase in the size of spray powder.

Erfanmanesh *et al.* [**22**] studied the effect of argon-shrouded plasma spray (ASPS) on the structure and properties of $MoSi_2$ coating. XRD analysis showed $MoSi_2$, MoO_3, SiO_2 and Mo_5Si_3 phases. Further, they observed that $MoSi_2$ coating exhibit less oxidation in ASPS as compare to atmospheric plasma spray (APS). Due to more oxidation of $MoSi_2$ coating, larger micro-cracks were obtained in APS. Therefore, lower cracks and fewer defects in ASPS method were observed. Moreover, the $MoSi_2$ coating through ASPS method demonstrated low porosity, highly homogeneous structure, large hardness and adhesion strength.

Yan *et al.* **[23]** synthesized $MoSi_2$ agglomerated powder for air plasma spraying (APS) through spray drying technique and sintering of powder. It was observed that $MoSi_2$ powder obtained by spray drying was spherical and porous. However, heat treatment of $MoSi_2$ powder resulted into decreased in porosity and sphericity of $MoSi_2$ particles. Moreover, flowability and apparent density of $MoSi_2$ powder was increased as compared to spray dry process when sintered at 1300 ^oC for 1hr.

Yeo *et al.* **[24]** synthesized $MoSi_2$ through self-propagating high temperature synthesis (SHS) using powder of molybdenum and silicon. The atomic ratio of Silicon to molybdenum was varied from 1.0 to 2.6. In SHS process value of atomic ratio of silicon to molybdenum (Si/Mo) such as 1.8, 2.0 and 2.2 showed stable combustion and single phase of $MoSi_2$ was obtained when Si/Mo ratio was 2.0. However, unstable combustion was observed when the Si/Mo ratio was less than 1.8 and greater than 2.2. This combustion constitute non-uniform and multi-phase products such as Mo, Si and Mo_5Si_3. XRD results revealed that Mo and Mo_5Si_3 appeared as major phase

when the Si/Mo ratio was 1 to 2.6. However, with increase in Si/Mo ratio, intensity of the major phases decreased and the intensity of $MoSi_2$ phase was increased.

Ovali *et al.* **[25]** synthesized $MoSi_2$ through mechnao-chemical process. They studied the effect of excess amount of reactants (MoO_3, SiO_2 and Mg) on the composition of mechano-chemically synthesized powder. It was observed that molybdenum phase was formed when excess amount of MoO_3 (20 wt %) was considered. However, content of Mo was decreased with excess amount of SiO_2 (20 wt%) and $MoSi_2$ phase appeared. Also, $MoSi_2$ phase was observed after the reduction of MoO_3 and SiO_2 by excess amount of Mg. XRD results revealed that molybdenum phase was decreased as the milling time of powder was increased.

Lu *et al.* **[26]** used Mo-Si-C, Mo-Si-Mo_2C and Mo-Si-SiC composite systems and synthesized $MoSi_2$ - 10 vol% SiC through self-propagating combustion method. XRD result showed the formation of $MoSi_2$ as primary product and SiC as secondary product in all composite system. In addition to these phases small amount of Mo_5Si_3 phase was also observed. However, $MoSi_2$-10 vol% SiC and $MoSi_2$ phases were formed at 1400ºC by vacuum hot pressing. They also observed that $MoSi_2$- 10 vol% SiC exhibits excellent mechanical properties prepared by Mo-Si-SiC composite system.

Samadzadeh *et al.* **[27]** studied the oxidation behavior of different materials based on $MoSi_2$ at low temperature (300 ºC-900 ºC). They considered different $MoSi_2$ heating elements of Kanthal Super (i.e. KS-1700, KS-1800, Ks-1900, KS-ER, KS-HT) at low temperature for 12 to 24 hrs. It was observed that oxidation of different material depends on exposure time and temperature, chemical and phase composition. KS-1700, KS-1800 and KS-ER possess better oxidation resistance up to 24 hrs against low temperature degradation whereas KS-1900 and KS-HT showed degradation at 300ºC-900 ºC after 24hrs.

Zhang *et al.* **[28]** studied the microstructure and oxidation behavior of Si-$MoSi_2$ coating on Mo substrate. They showed that three layers were formed such as surface layer (Si-$MoSi_2$), intermediate layer ($MoSi_2$) and transitional layer (Mo-Mo_5Si_3- Mo_3Si) by Si-$MoSi_2$ coating on Mo substrate through liquid phase siliconizing method. The surface layer consists of highest silicon content (i.e.50 wt%). Also they observed that silicon content was reduced with increased in diffusion depth. The silicon content in intermediate layer was 30-34 wt%. However, it showed no change with increased in diffusion depth. This resulted into the formation of $MoSi_2$. Further,

transitional layer (called low silicon content layer) showed sharp decreased in silicon with increased in diffusion depth. Mo and low silicon silicides (Mo_3Si, Mo_5Si_3) were observed in this layer. Also, they showed that large amount of silicon content at surface layer reduced the formation of Mo_5Si_3 and MoO_3 phases.

Zhang *et al.* **[29]** prepared $MoSi_2$ by reacting molybdenum disulfide (MoS_2) and silicon (Si). This reaction resulted into two silicide compounds (i.e. $MoSi_2$ and Mo_5Si_3) and sulfide compound such as SiS. However, $MoSi_2$ and SiS phases were formed with 1:4 molar ratio of MoS_2 to Si in temperature range 0 ºC -1700ºC. They observed that pure $MoSi_2$ phase was obtained at 1363ºC after the phase transformation of SiS sublimate to gaseous phase in 2hrs. However, pure $MoSi_2$ was not observed at 900 ºC in duration of 12hrs due to slow reaction rate between MoS_2 and Si. Also, they observed that grain size of $MoSi_2$ product increases with increased temperature.

REFERENCES

[1] S. Zhang, Z. A. Munir, *Synthesis of molybdenum silicides by self-propagating combustion method,* Journal of Materials Science 26 (1991) 3685-3688.

[2] R.B. Schwarz, J.J. Petrovic, C.J. Maggoire, *Synthesis of molybdenum disilicide by mechanical alloying,* Materials Science and Engineering A155 (1992) 75-83.

[3] B.K. Yen, T. Aizawa, J. Kihara, *Synthesis and formation mechanisms of molybdenum silicides by mechanical alloying,* Materials Science and Engineering A220 (1996) 8-14.

[4] H. Shimizu, M. Yoshinaka, K. Hirota, *Fabrication and mechanical properties of monolithic Mosi$_2$ by spark plasma sintering,* Materials Research Bulletin 37 (2002) 1557-1563.

[5] G. Wang, W. Jiang, *Effect of addition of oxides on low- temperature oxidation of molybdenum disilicide,* Journal of the American Society 86 (2003) 731-734.

[6] Xu. Jianguang, Z. Baolin, L. Wenlan, *Synthesis of pure molybdenum disilicide by chemical oven self-propagating combustion method,* Ceramics International 29 (2003) 543-546.

[7] J. Kuchino, K. Kurokawa, T. Shibayama, *Effect of microstructure on oxidation resistance of MoSi$_2$ fabricated by spark plasma sintering,* Vacuum Surface Engineering, Surface instrumentation and vacuum technology 73 (2004) 623-628.

[8] J.N. Woolen, J.J. Petrovic, Z.A. Munir, *Micro-alloying of molybdenum disilicide with magnesium through mechanical and field activation,* Journal Of Materials Science 39 (2004) 5037-5043.

[9] M. Zakeri, R.Y.Rad, M.H. Enayati, *Synthesis of nano-crystalline MoSi$_2$ by mechanical alloying,* Journal of Alloys and Compounds 403 (2005) 258-261.

[10] F. Zhang, L. Zhang, A. Shan, J. Wu, *Oxidation of stoichiometric poly- and single-crystalline MoSi$_2$ at 773K,* Intermetallics 14 (2006) 406-411.

[11] J. Xu, H. Zhang, J. Yan, B. Zhang, W. Li, *Effect of argon atmosphere on the formation of MoSi$_2$ by self- propagating combustion method,* International Journal of Refractory Metals and Hard Materials 25 (2007) 318-321.

[12] G. Cabouro, S. Chevalier, E. Gaffet, Y. Grin, F. Bernard, *Reactive sintering of molybdenum disilicide by spark plasma sintering from mechanically activated powder mixtures: Processing parameters and properties,* Journal of alloys and Compounds 465 (2008) 344-355.

[13] F. Zhong, W. Hong, Q. Huai, Q. Xuan, *Energy analysis of mechanical alloying of molybdenum disilicide in a new- type high energy vibrating ball mill,* Journal of China university of Mining and Technology 18 (2008) 0449-0453.

[14] P. Feng, X. Qu, F. Akhtar, X. Du, C. Jia, *Effect of the composition of starting materials of Mo-Si on the mechanically induced self-propagating reaction,* Journal of Alloys and Compounds 456 (2008) 304-307.

[15] H. Nersisyan, H. Won and C.W. Won, *Combustion synthesis of molybdenum disilicide ($MoSi_2$) Fine powders,* Journal of American Society 91 (2008) 2802-2807.

[16] M.S. Khoshkoo, M. Shamanian, A. Saidi, M.H. Abbasi, *The effect of Mo particle size on SHS synthesis mechanism of $MoSi_2$,* Journal of Alloys and Compounds 475 (2009) 529-534.

[17] P. Feng, A. Farid, X. Wang, W. Liu, J. Wu and S. Zhang, *Effect of diluents on the synthesis of molybdenum disilicide by mechanically-induced self- propagating reaction*, Journal of Alloys and Compounds 494 (2010) 301-304.

[18] G. Cabouro, S.L. Gallet, S. Chevalier, E. Gaffet, Yu. Grin, F. Bernard, *Dense $MoSi_2$ produced by reactive flash sintering: Control of Mo/Si agglomerates prepared by high-energy ball milling,* Powder Technology 208 (2011) 526-531.

[19] T. Yamada, H. Yamane, *Low temperature synthesis of α-MoS_2 and β-$MoSi_2$ powders using Na,* Journal of alloys and Compound 509 (2011) 123-125.

[20] S. Hasani, M. Panjepour, M. Shamanian, *Effect of atmosphere and heating arte on the mechanism of $MoSi_2$ formation during self- propagating high-temperature synthesis*, Journal of Thermal Analysis Calorimetry 107 (2012) 1073-1081.

[21] J. Yan, I. Liu, Z. Mao, H. Xu and Y. Wang, *effect of spraying Powder size on the microstructure, bonding strength, and micro-hardness of $MoSi_2$ coating prepared by Air Plasma Spraying,* Journal of Thermal Spray Technology 23 (2014) 934-939.

[22] M. Erfanmanesh, S.R. Bakhshi, M. Khajelakzay, M. Salebafghi, *the effect of argon shielding gas at plasma spray process on the structure and properties of $MoSi_2$ coating,* Ceramics International 40 (2014) 4529-4533.

[23] J. H. Yan, J.J. Xu, Y. Wang, *preparation of agglomerated powders for air plasma spraying $MoSi_2$ coating,* Ceramics International 41 (2015) 10547-10556.

[24] S.C. Yeo, S. W. Jeon, J.E. Lee, *Combustion characteristics of molybdenum-silicon mixtures,* Ceramics International 41 (2015) 1711-1723.

[25] D. Ovali, D. Agaogullari, M L. Ovecoglu, *Effects of excess reactant amounts on the mechano-chemically synthesized molybdenum silicides from MoO_3, SiO_2 and Mg blend,* International Journal of Refractory Metals and Hard Materials 65 (2016) 19-24.

[26] Q. Lu, G. Zhu, X. Wang, Z. Wang, P. Feng, *Effects of Raw Materials on Synthesis, Microstructure and Properties of MoSi2-10 Vol% SiC Composites,* Transactions of the Indian Ceramic Society 75 (2016) 33-39.

[27] M. Samadzadeh, C. Oprea, H. K. Sharif, *Comparative studies of the oxidation of $MoSi_2$ based materials : Low-temperature oxidation (300-900ºC),* International Journal of Refractory Metals and Hard Materials 66 (2017) 11-20.

[28] Y. Zhanga, Y. Lib, C. Bai, *Microstructure and oxidation behavior of Si–MoSi2 functionally graded coating on Mo substrate,* Ceramics International 43 (2017) 6250-6256.

[29] G.H. Zhang, G.D. Sun, K.C. Chou, *A novel process to prepare MoSi2 by reaction between $MoSi_2$ and Si,* Journal of Alloys and Compounds 694 (2017) 480-488.

3.1. Raw materials

In the present study, $MoSi_2$ was synthesized using raw chemicals, molybdenum trioxide (99%, *Loba Chemie*), silicon dioxide (99%, *Loba Chemie*), silicon (99.9%, Sigma Aldrich) magnesium (99%, *S.D. Fine Chemicals*) and hydrochloric acid (99%, *S.D. Fine Chemicals*). All chemicals were used as such without any further purification.

3.2. Sample preparation

The synthesis route followed to prepare $MoSi_2$ has been categorized on the basis of silicon source used in the present study. The experimental details are presented in the flow chart (Fig. 3.1). In the first series, silicon dioxide was used as the source of silicon, which was mixed with molybdenum trioxide and magnesium.

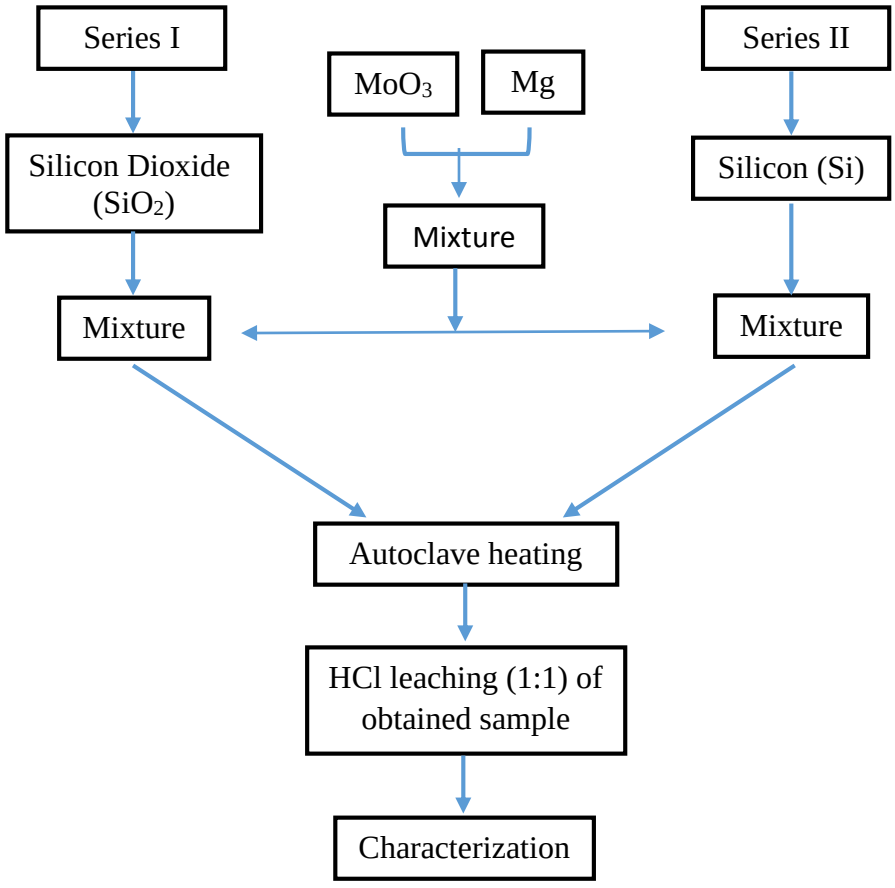

Fig. 3.1 Flow chart of $MoSi_2$ synthesis.

The role of magnesium is crucial because it helps in the reduction of oxides. Afterwards, the mixed sample were charged into a specially designed autoclave. The autoclave was purged with high purity argon, in order to avoid oxidation of the sample. Further, this autoclaved was

sealed and placed in an electric furnace at room temperature and heated at 5 ºC/min heating rate. The samples were heated at desired temperature and then maintained for different intervals of time. The schematic diagram of synthesis route for $MoSi_2$ is presented in figure 3.2.

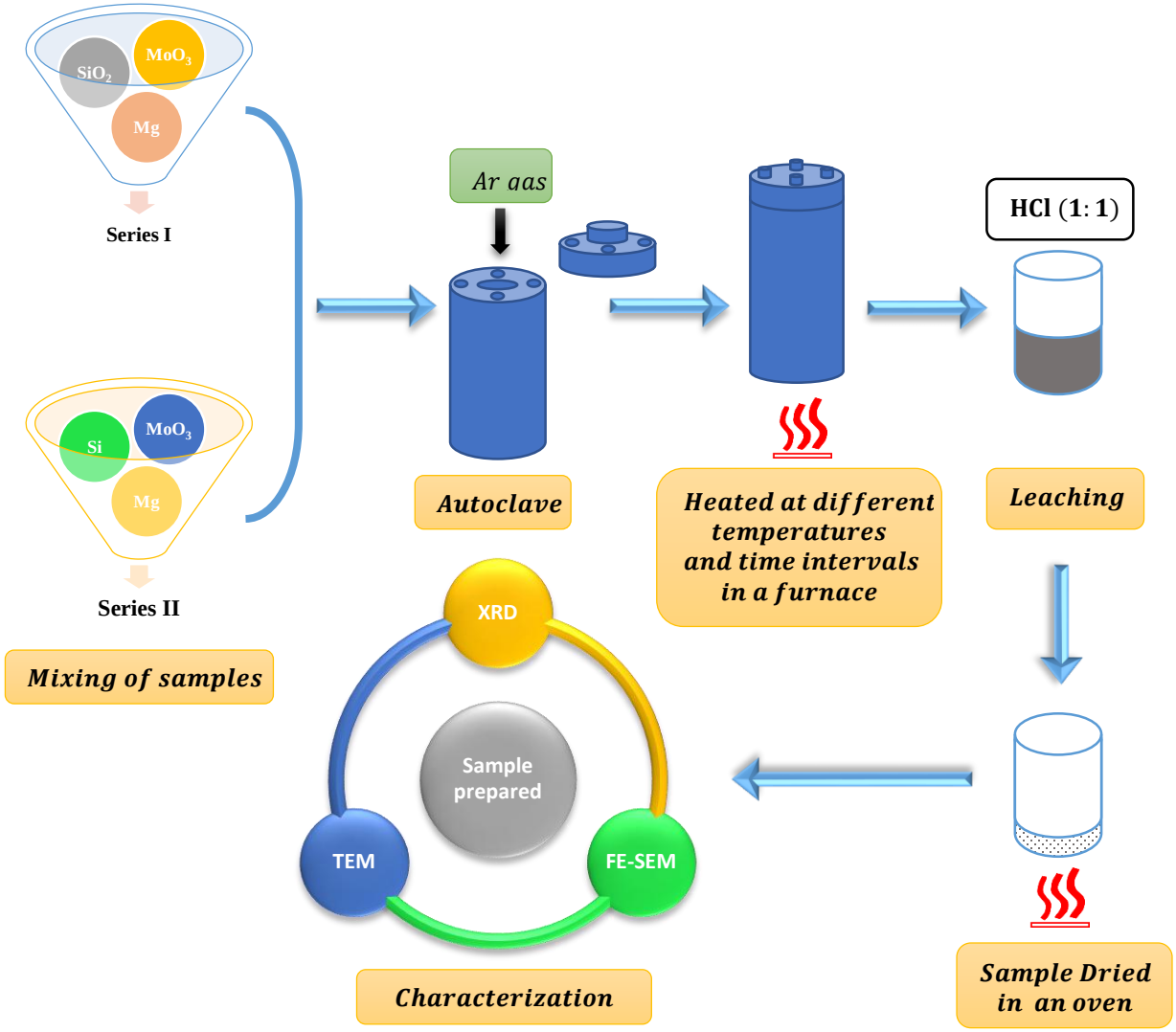

Fig. 3.2 Schematic diagram of synthesis route for $MoSi_2$.

Similarly, in the second series, pure silicon was used as silicon source and rest remains the same. This method also follows the same synthesis route as of first one. The initial composition and labelling of all the samples prepared in series I and series II are listed in table 3.1 and table 3.2, respectively.

Table 3.1 The initial composition and sample ID of all samples in series I.

SERIES I					
Sample ID	**Precursors**			**Temperature (ºC)**	**Duration (hrs)**
	MoO_3 **(**mol**)**	SiO_2 (mol)	Mg (mol)		
MS1	1	2	12	800	10
MS2	0.5	2	12	800	15
MS3	0.5	2	12	900	10
MS4	0.5	2	12	900	15

Table 3.2: The initial composition and sample ID of all samples in series II.

SERIES II					
Sample ID	**Precursors**			**Temperature (ºC)**	**Duration (hrs)**
	MoO_3 **(**mol**)**	Si (mol)	Mg (mol)		
MS5	1	2	3	800	0
MS6	1	2	3	800	5
MS7	1	2	3	800	10
MS8	1	2	3	800	15
MS9	1	2	4	800	15
MS10	1	2	4	800	20
MS11	1	2	4	900	10
MS12	1	2	4	900	15

3.3. Material Characterization

3.3.1. X-ray Diffraction (XRD)

In this work, XRD of all the samples were studied through *PANalytical Xpert-Pro* having Cu-Kα radiation ($\lambda = 1.54$ Å) obtained from Cu target material. The generator operating was kept at 45 kV and 40 mA. All the diffractograms were obtained in the defined range of 2θ i.e. 20º – 80º having a step size of 2θ = 0.0130º, at room temperature. Initially, all the prepared samples were ground in an agate mortar pistle for 30 min, in order to achieve uniform particle size distribution, before XRD. These diffractograms were further analysed with the help of *X'Pert Highscore* Plus software and all the observed peaks were marked with reference to International Centre of Diffraction Data (ICDD) cards.

3.3.2. Field Emission Scanning Electron Microscopy (FE-SEM)

The morphology of the best prepared samples was studied with the help of FESEM. The sample preparation for FE-SEM is important to get good results. The samples before FESEM were properly grounded in an agate mortar for 1 hr. and heated in an oven for 12 hrs. at 100 ºC to remove moisture content. The prepared samples were analysed through Merlin Compact model make of Carl Zeiss. The micrographs of the samples were obtained at different magnifications.

3.3.3. Transmission Electron Microscopy (TEM)

The structure of best sample below atomic level was investigated through TEM. In order to obtain good results, sample preparation for TEM is highly crucial. The sample prepared for TEM must be very thin (<100 nm) to transmit electron from the sample and increases the spatial resolution imaging. In addition, high resolution transmission electron microscopy (HR-TEM) was performed to measure lattice fringes. The sample was analyzed through JEOL 2100F operating at 200 kV. Firstly, the sample was dispersed in ethanol through ultrasonication for 30 min and then dispersed sample was dropped on a TEM grid made of carbon coated copper. The sample was allowed to dry at room temperature and hence, sample is prepared for TEM analysis.

4.1. Synthesis of molybdenum disilicide ($MoSi_2$) from series I

4.1.1. XRD analysis of Series-I samples

Fig. 4.1 shows the XRD of non-leached (Fig. 4.1a) and leached (Fig. 4.1b) MS1 sample. It is observed from figure 4.1a that magnesium oxide along with molybdenum, silicon and silicon dioxide are present in non-leached MS1 sample. In order to remove unwanted phase of MgO, leaching of MS1 sample was done. Figure 4.1b clearly indicates that the unwanted phase of MgO is completely removed from MS1 sample after leaching. It is also observed from this figure that molybdenum (Mo) metal is in major phase and other phases i.e. silicon dioxide (SiO_2), molybdenum oxide (Mo_4O_{11}) and silicon (Si) are also observed. This indicates that the MoO_3 is significantly reduced to Mo with help of Mg.

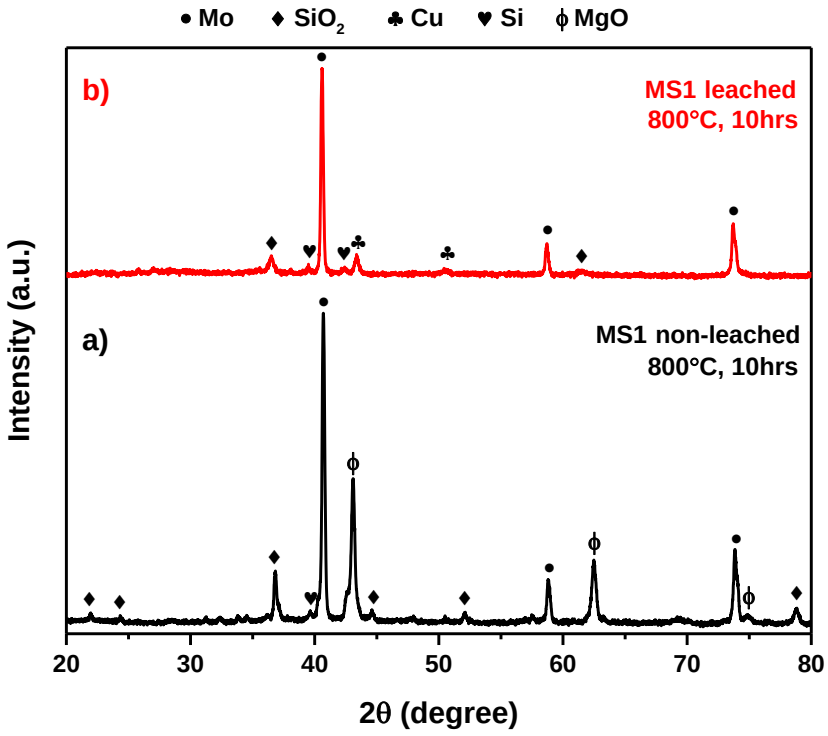

Fig. 4.1 XRD of (a) non-leached and (b) leached MS1 sample.

In addition, there is no complete reduction of oxides (MoO_3, SiO_2) has occurred. This might be associated with the choice of initial composition of MS1 for the synthesis of $MoSi_2$. The formation of $MoSi_2$ phase is not observed due to less amount of silicon dioxide and magnesium in

the initial composition. Similar, results were also obtained by Ovali *et.al* **[1]** and they concluded that excess amount of molybdenum trioxide leads to the formation of molybdenum metal.

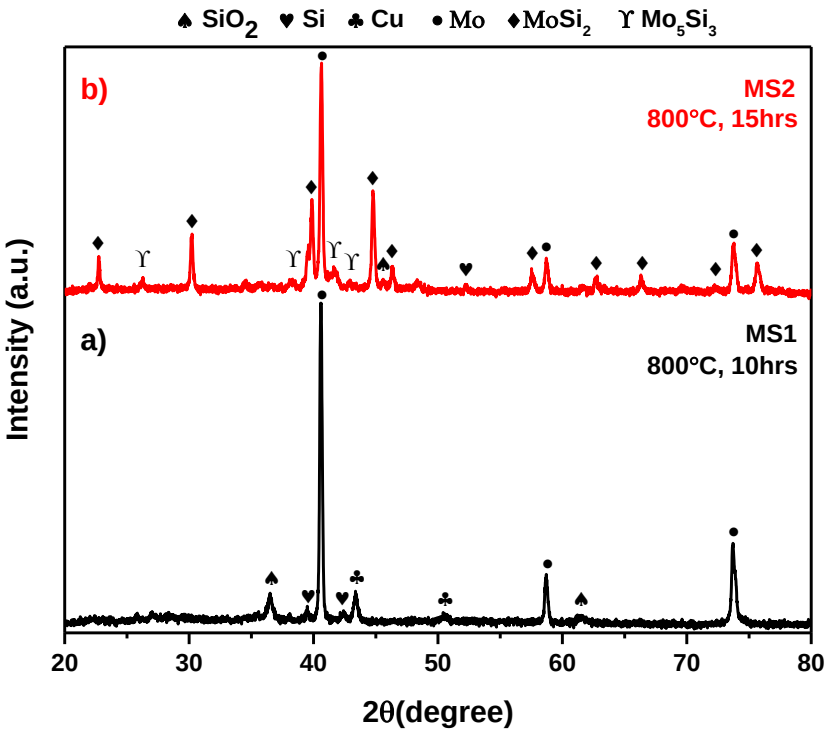

Fig. 4.2 XRD of (a) MS1 and (b) MS2 samples.

Further, for complete reduction of oxides (MoO_3, SiO_2) and to obtain $MoSi_2$, the content of MoO_3 was reduced in MS2 (Fig. 4.2b). Also, this sample was heated at for 15 hrs. at 800 ºC temperature. The presence of molybdenum during increase in duration of sample (10hrs to 15hrs) leads to the formation of molybdenum rich silicide (Mo_5Si_3) **[2]**. This comparative figure (Fig. 4.2) shows that the decrease in MoO_3 resulted into formation of $MoSi_2$ in the major phase. However, still there is oxide content in higher amount, so, further optimization was done to get single phase $MoSi_2$. Moreover, it is observed that Mo and Si phases are present designating that complete reaction between Mo and Si is not achieved. Therefore, temperature was increased in MS3 (Fig. 4.3a) and MS4 (Fig. 4.3b) samples to accomplish complete reaction between Mo and Si.

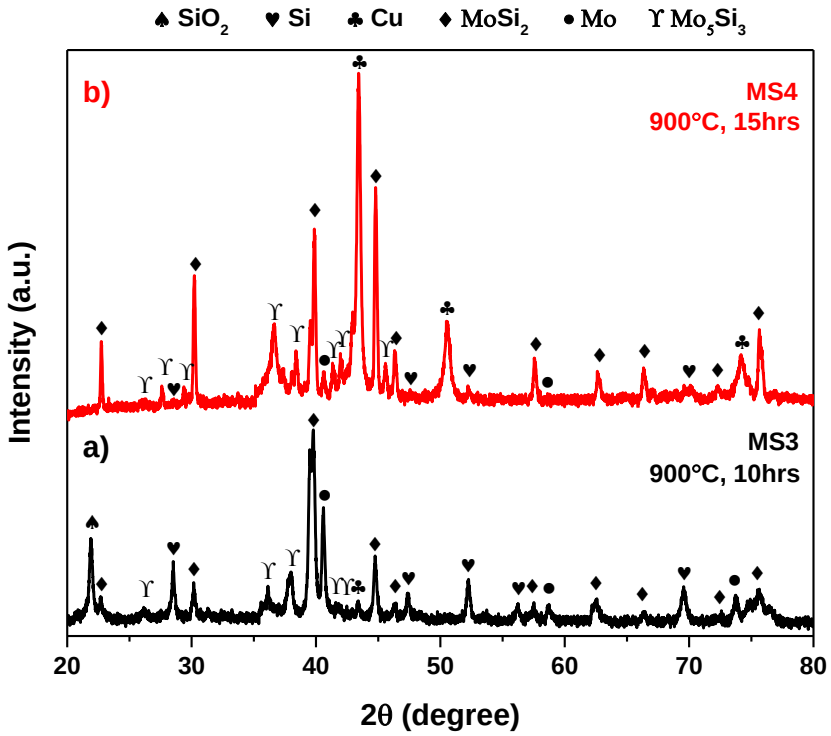

. **Fig. 4.3** XRD of (a) MS3 and (b) MS 4 samples.

It is observed from figure 4.3 that increase in temperature resulted into melting of copper gasket employed to seal the autoclave. In both samples (MS3-MS4), traces of Cu metal are obtained with Mo_5Si_3, $MoSi_2$, Si and SiO_2. As the duration increased to 15 hrs. in MS4 sample the peaks associated with Cu metal become more pronounced as compared to MS3 sample. Although, the content of $MoSi_2$ is increased in MS4 sample but melting Cu leads to failure of this experiment. Therefore, the precursor of silicon was changed from SiO_2 to Si pure to obtain $MoSi_2$.

4.2. Synthesis of molybdenum disilicide ($MoSi_2$) from series II

4.2.1. XRD analysis of series II samples

Fig 4.4 – 4.5 shows the XRD of leached MS5-MS8 samples heated at 800 ºC for different time intervals (0, 5, 10, 15 hrs.). It is observed from Fig. 4.4a that there is complete reduction of MoO_3 to Mo metal and no reaction started in between Si and Mo. A very small peak associated with SiO_2 is observed indicating oxidation of Si. There is no change observed when the duration of heating is increased to 5 hrs. (Fig. 4.4b) in MS6 sample. Since, no reaction occurred between Mo and Si at 800 ºC up to 5hrs.duration. Therefore, the formation of $MoSi_2$ is investigated at 800

ºC for 10 hrs. (Fig. 4.5a) and 15 hrs. (Fig. 4.5b) time intervals in MS7 and MS8 samples, respectively.

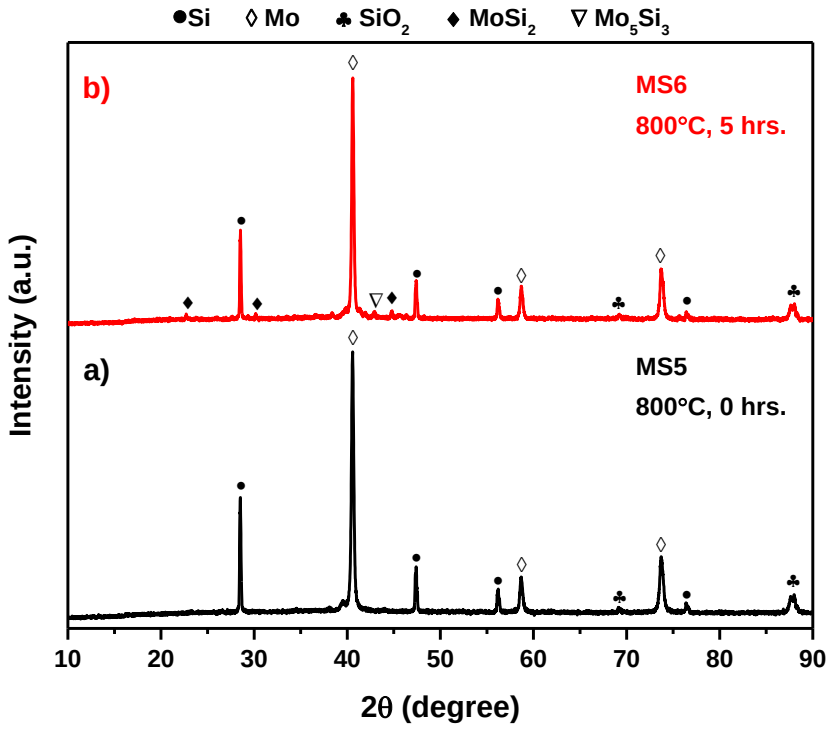

Fig. 4.4 XRD of (a) MS5 and (b) MS6 samples heated at 800 ºC for 0 hr. and 5 hrs. duration.

Fig. 4.5a shows the XRD of MS7 sample heated at 800 ºC for 10 hrs. duration. This figure demonstrated that the reaction between Mo and Si is favored and peaks associated with $MoSi_2$ and Mo_5Si_3 appeared. Also, MS8 sample shows more pronounced peaks of $MoSi_2$ and Mo_5Si_3, when the heating duration was increased to 15 hrs. (Fig. 4.5b) at 800 ºC. However, no complete reaction is achieved at this stage. Moreover, Ovali *et.al* **[1]** also investigated the impact of composition on the formation $MoSi_2$. They suggested that excess MoO_3 and Si results into more Mo metal and formation of $MgSiO_2$ and $MgSi_2$ phases. Also, the Mg content plays a crucial role in the formation of $MoSi_2$. The excess amount Mg favors the formation of $MoSi_2$ phase because it enhances the reduction of oxide phases and prompts the reaction between Mo and Si to form $MoSi_2$.

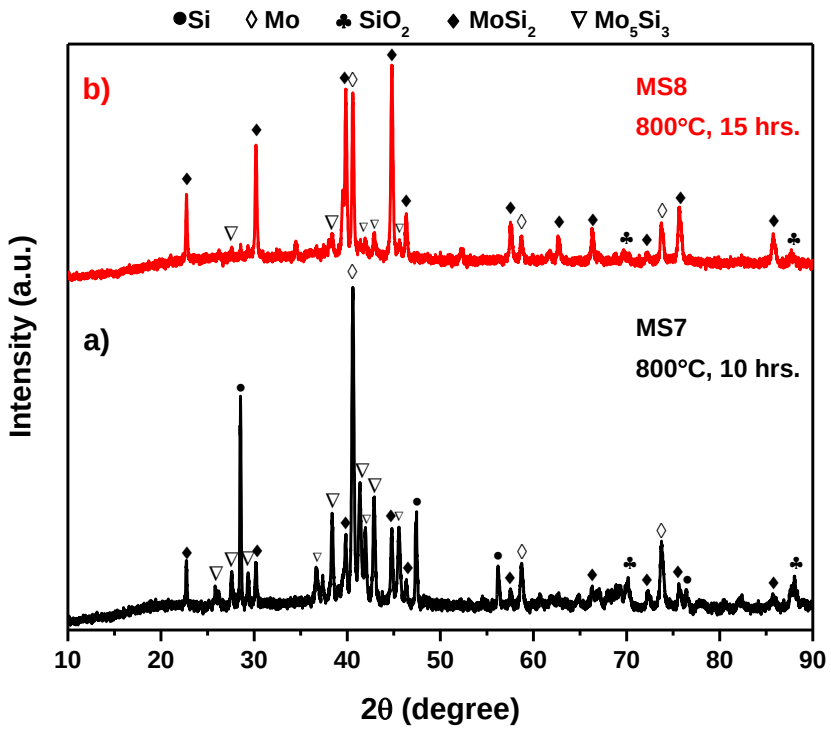

Fig. 4.5 XRD of (a) MS7 and (b) MS8 samples heated at 800 ºC for 10 hrs. and 15 hrs. duration.

In the present study, there is no formation of $MgSiO_2$ and $MgSi_2$ phases observed designating that the content of Si seems to be optimum. In addition, no reaction occurred between Mo and Si at 800 ºC up to 5hrs. duration. Therefore, the content of Mg must be increased in MS9-MS10 samples to favor the formation of $MoSi_2$. These samples were heated at 800 ºC for 15 hrs. and 20 hrs. time intervals.

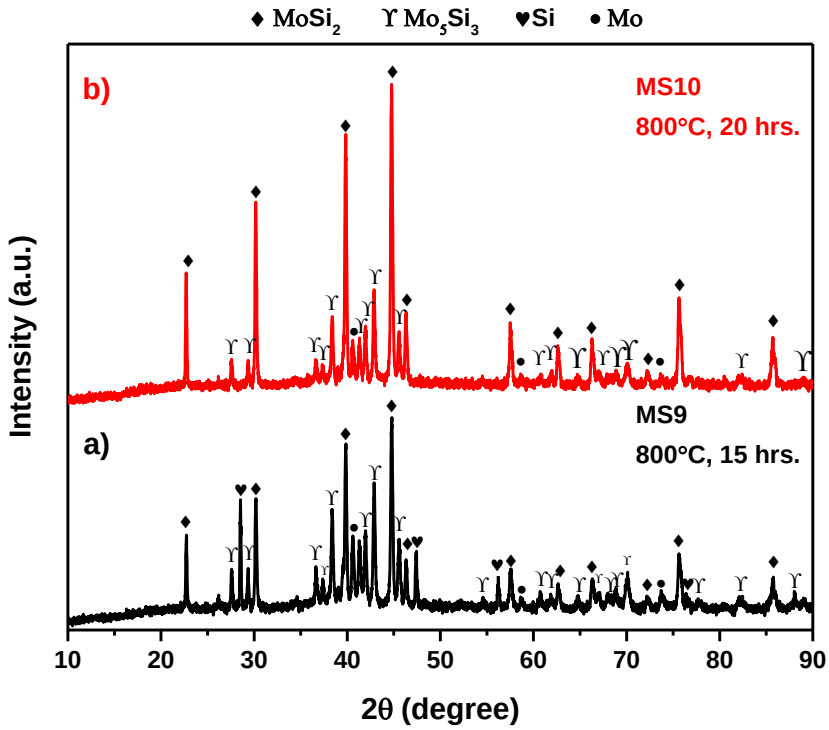

Fig. 4.6 XRD of (a) MS9 and (b) MS10 samples heated at 800 ºC for 15 hr. and 20 hrs. duration.

The XRD of MS9 sample heated at 800 ºC for 15 hrs. (Fig. 4.6a) reveals that there is formation of $MoSi_2$, Mo_5Si_3, Mo and Si phases. As the dwell time increased to 20 hrs. in MS10 sample (Fig. 4.6b), the intensity of peaks associated with Mo and Mo_5Si_3 decreased. Also, Si peak completely disappeared with increase in dwell time (20 hrs.) **[3,4]**. Furthermore, the intensity of peaks related to $MoSi_2$ are increased. This clearly indicates that the increment in Mg content and increased time duration favors the formation of $MoSi_2$. Xu *et al.* **[5]** also suggested that the content of Mo decreased and $MoSi_2$ increase with increase in duration. Furthermore, Kang *et al.* **[6]** studied the impact of temperature and concluded that the formation of $MoSi_2$ increases and the content of Mo, Si and Mo_5Si_3 decreases.

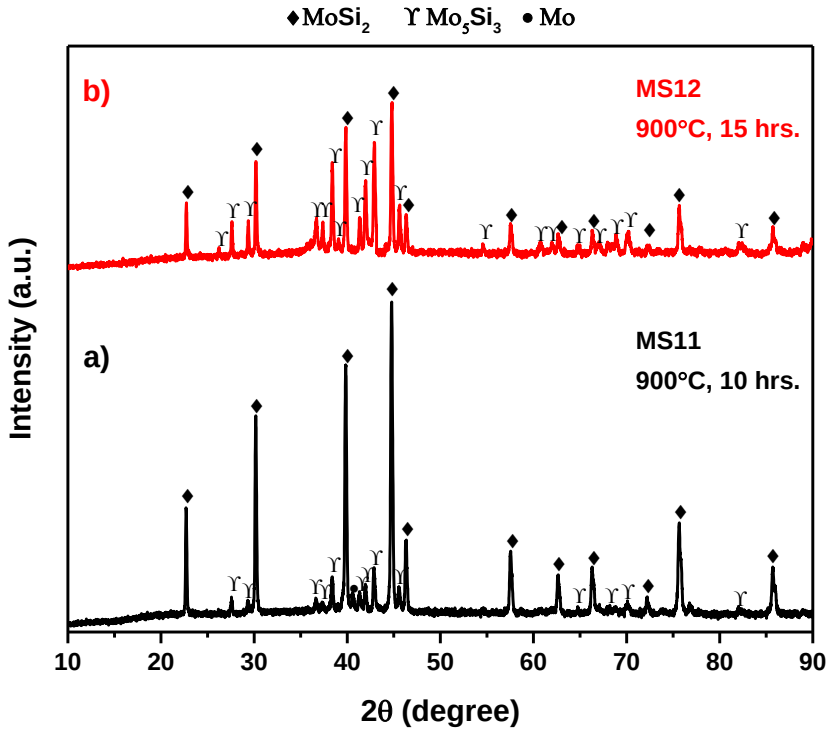

Fig. 4.7 XRD of (a) MS11 and (b) MS12 samples heated at 900 ºC for 10 hrs. and 15 hrs. duration.

Moreover, the content of Mg and reaction temperature was further increased in MS11-MS12 samples (Fig. 4.7) to investigate the formation of $MoSi_2$. It is observed from figure 4.7a that the $MoSi_2$ phase emerge as major phase in the XRD obtained for MS11 sample heated at 900 ºC for 10 hrs. dwell time. When the duration increased to 15 hrs. in MS12 sample, Mo_5Si_3 phase became more pronounced as compared to 10hrs. dwell time **[8]**. This clearly reveals that the $MoSi_2$ phase starts to decompose with increase in dwell time at 900 ºC. Therefore, best results associated with the formation $MoSi_2$ are observed by increasing Mg content to 30% and heating sample at 900 ºC for 10 hrs. of dwell time.

4.3. FE-SEM analysis

The surface morphology of best prepared samples is studied through FE-SEM. Fig. 4.8-4.9 shows the micrograph of MS10-MS11 sample heated at 800 ºC and 900 ºC for 20 hrs. and 10 hrs. dwell time, respectively. These figures clearly demonstrate that the particles are agglomerated and distribution of the particles is not homogeneous.

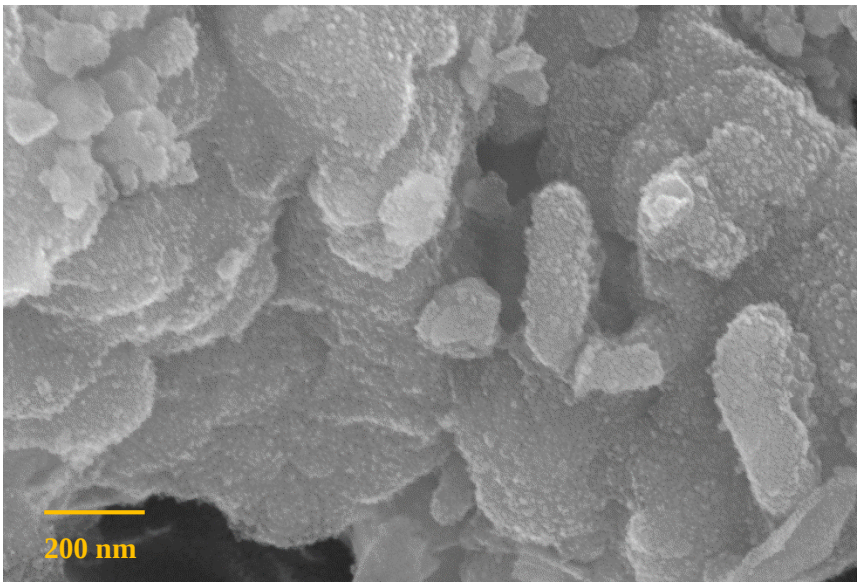

Fig. 4.8 Micrograph of molybdenum disilicide synthesized at 800ºC for 20 hrs. dwell time.

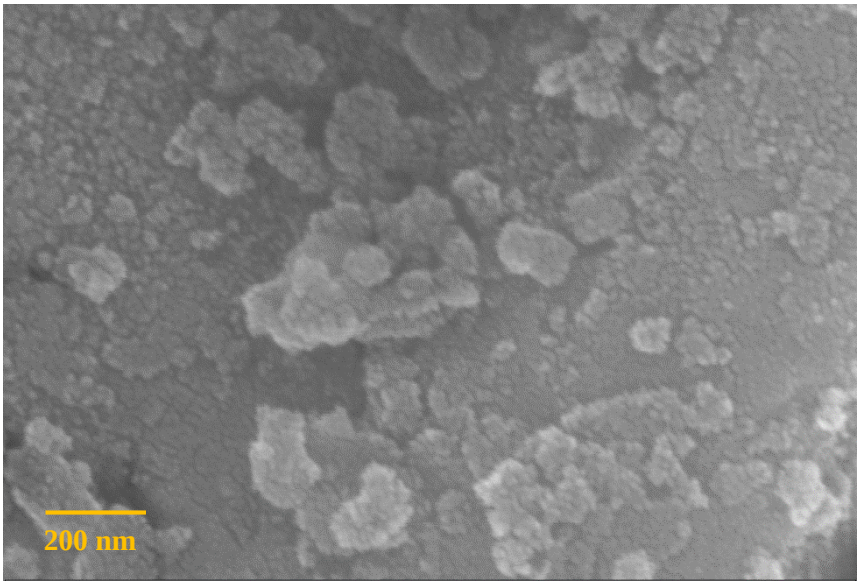

Fig. 4.9 Micrograph of molybdenum disilicide synthesized at 900ºC for 10 hrs. dwell time.

Also, the shape of the particles is irregular and each particle possess different shapes. The agglomeration of the particles might be due to heat released during exothermic reaction **[9]**. It is observed that the particle and agglomerates size is reduced when the dwell time is 20hrs as compare to 10hrs. Therefore, it is concluded that particle size decreased as the dwell time of the sample is increased. Similar, results are also observed by Zakeri *et.al* **[10]**. They observed that particles and agglomerated particle size reduced increase in dwell time.

4.4. HR-TEM analysis

The HR-TEM image represents the spacing of lattice fringe which corresponds to particular plane of molybdenum disilicide crystal. The spacing of lattice fringe was observed 0.22 nm in figure 4.10. This spacing of lattice fringe matched with the plane (103) of molybdenum disilicide ($MoSi_2$) corresponding to standard card (01-081-2167). The results are in agreement with XRD results and this confirms the formation of $MoSi_2$ phase.

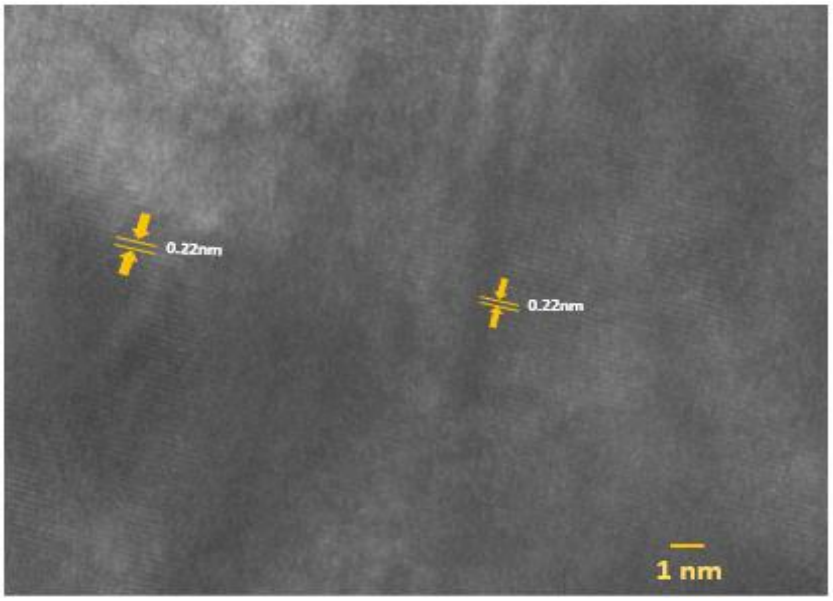

Fig. 4.10 HR-TEM of molybdenum disilicide synthesized at 900ºC for 10 hrs. dwell time

4.4. Formation mechanism of $MoSi_2$

4.4.1. Series I

The formation mechanism of molybdenum disilicide follows multistep process (i.e. reduction and silicidation) in an autoclave. In the present study MoO_3 act as the molybdenum source while magnesium act as reducing agent.

The following steps takes place in an autoclave

1. Reduction of MoO_3 to Mo with Mg
2. Silicidation of Mo with Mg and SiO_2 to Mo-Si compounds (Mo_5Si_3 ,$MoSi_2$) and Si
3. Direct reduction- silicidation of MoO_3 to Mo-Si Compounds

I) Reduction of MoO_3 to Mo with SiO_2 and Mg

The following reaction path given below shows the reduction of MoO_3 to Mo in an autoclave

$$MoO_3 + SiO_2 + 5Mg \rightarrow Mo + 5MgO + Si \quad (4.1)$$

Magnesium being highly reactive absorbs oxygen from autoclave to form MgO, which act as catalyst for the formation of $MoSi_2$ **[10]**. The variation of ΔH at different temperature is shown in Fig 4.11, which shows that ΔH has positive value and predicts that there is less possibility of the formation of Mo in presence of SiO_2. However, with increase in temperature ΔH decreases from 57.4 kJ to 30.2 kJ. So, reduction of MoO_3 to Mo is possible.

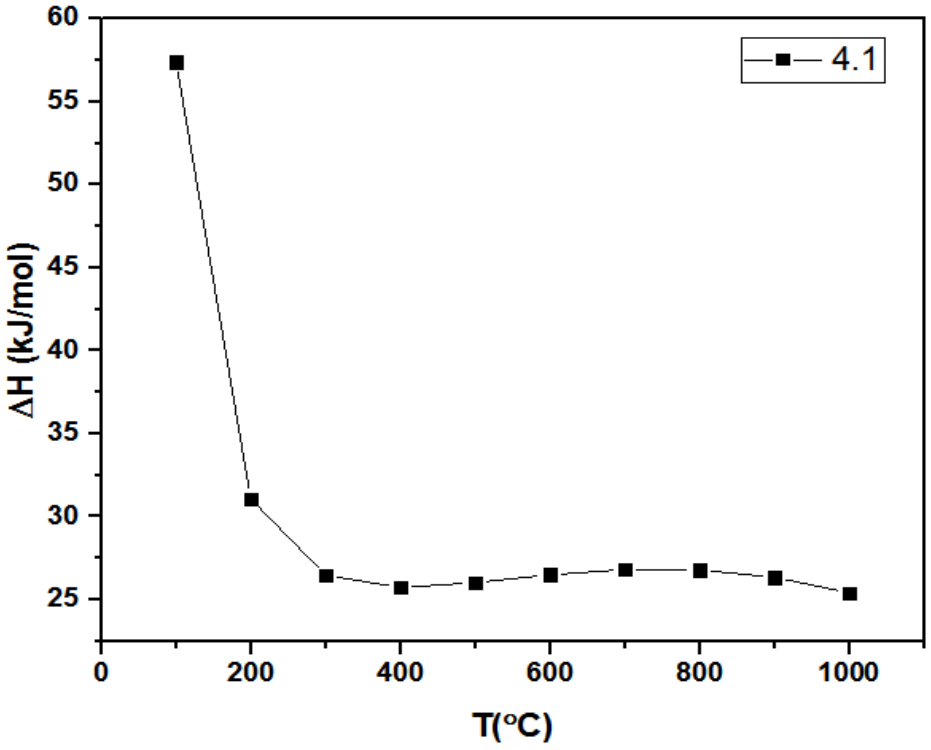

Fig 4.11 Variation of ΔH at different temperature

II) Silicidation of Mo with Mg and SiO_2

Following reaction path ways have been framed for silicidation of Mo to Mo-Si compounds (Mo_5Si_3 and $MoSi_2$) in presence of Mg and SiO2in an autoclave.

$$Mo + 2SiO_2 + 4Mg \rightarrow MoSi_2 + 4MgO \quad (4.2)$$

$$5Mo + 3SiO_2 + 6Mg \rightarrow Mo_5Si_3 + 6MgO \quad (4.3)$$

$$6Mo + 5SiO_2 + 10\,Mg \rightarrow MoSi_2 + Mo_5Si_3 + 10MgO \quad (4.4)$$

$$Mo + 3SiO_2 + 6Mg \rightarrow MoSi_2 + 6MgO + Si \quad (4.5)$$

$$5Mo + 4SiO_2 + 8MgO \rightarrow Mo_5Si_3 + Si + MgO \quad (4.6)$$

$$6Mo + 6SiO_2 + 12Mg \rightarrow MoSi_2 + Mo_5Si_3 + \quad 12MgO + Si \qquad (4.7)$$

The ΔH variation with temperature of above reactions is shown in Fig 4.12. The ΔH variation is positive with temperature. However, reaction 4.7 has least positive value at different temperatures among the reactions 4.2 to 4.7, respectively. The positive trend of ΔH with temperature confirms there is less possibility of formation of Mo-Si compounds from the given reaction path ways.

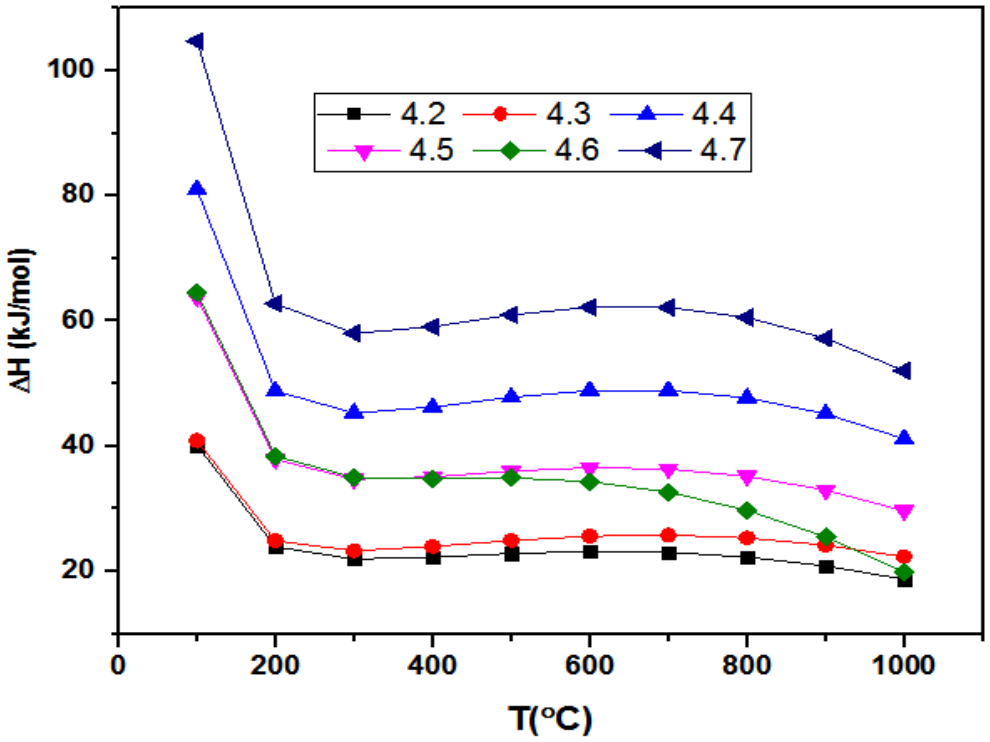

Fig 4.12 Variation of ΔH at various temperature

III) Reduction-Silicidation Of MoO_3 to Mo-Si compounds (Mo_5Si_3, $MoSi_2$)

The possible reaction path ways framed for the formation of molybdenum silicides from MoO_3 in the presence of Mg and SiO_2 in an autoclave is shown below:

$$MoO_3 + 2SiO_2 + 7Mg \rightarrow MoSi_2 + 7MgO \qquad (4.8)$$

$$5MoO_3 + 3SiO_2 + 21Mg \rightarrow Mo_5Si_3 + 21MgO \qquad (4.9)$$

$$6MoO_3 + 5SiO_2 + 28MgO \rightarrow MoSi_2 + Mo_5Si_3 + 28MgO \qquad (4.10)$$

$$MoO_3 + 4SiO_2 + 23Mg \rightarrow Mo_5Si_3 + Si + 23MgO \qquad (4.11)$$

$$MoO_3 + 2SiO_2 + 9Mg \rightarrow MoSi_2 + 9MgO + Si \qquad (4.12)$$

$$6MoO_3 + 6SiO_2 + 30Mg \rightarrow MoSi_2 + Mo_5Si_3 + 30MgO + Si \qquad (4.13)$$

$$Mo_5Si_3 + 7SiO_2 + 14Mg \rightarrow 5MoSi_2 + 14MgO \quad (4.14)$$

The ΔH variation with temperature of above given reactions is shown in Fig. 4.13, which also shows the positive value of ΔH. This confirms that there is less possibility of formation of $MoSi_2$ in presence of SiO_2. The results are in accordance with that observed in XRD. The high affinity of oxygen diffusion at higher temperature results in formation of SiO_2 without formation of pure phase of $MoSi_2$. To attain a single phase $MoSi_2$, the silicon source was changed from SiO_2 to pure Si.

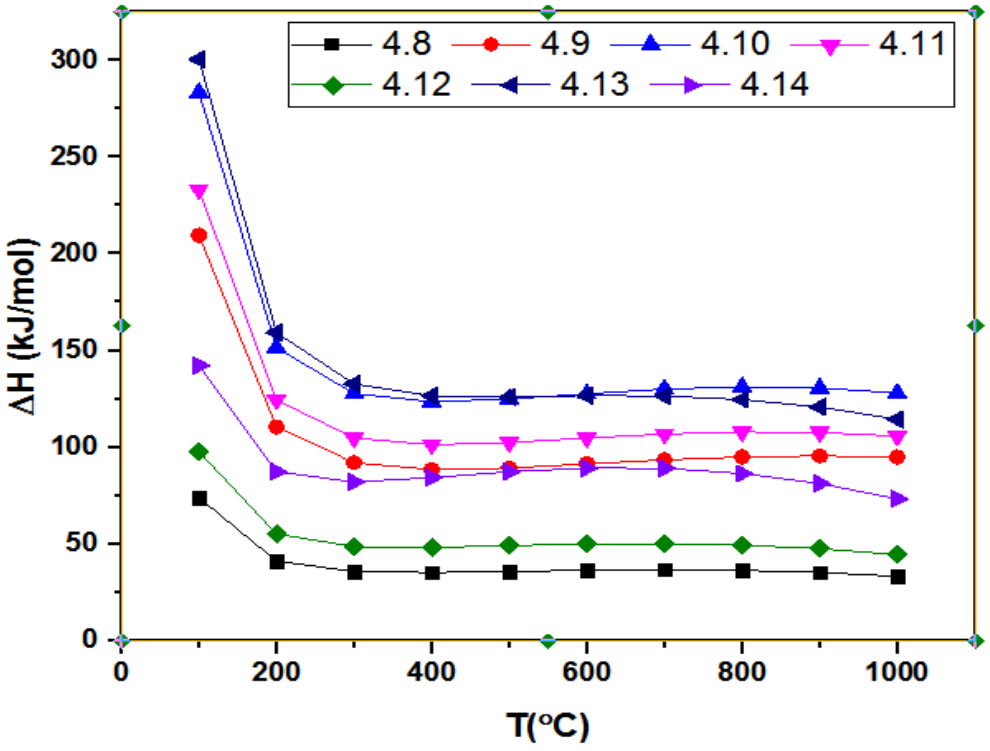

Fig 4.13 Variation of ΔH at different temperature

The above reactions show the positive value of ΔH at different temperature. So, it can be concluded that there is less possibility of formation of $MoSi_2$ in the presence of SiO_2. Therefore, in order to attain a single phase $MoSi_2$, the silicon source was changed from SiO_2 to pure Si.

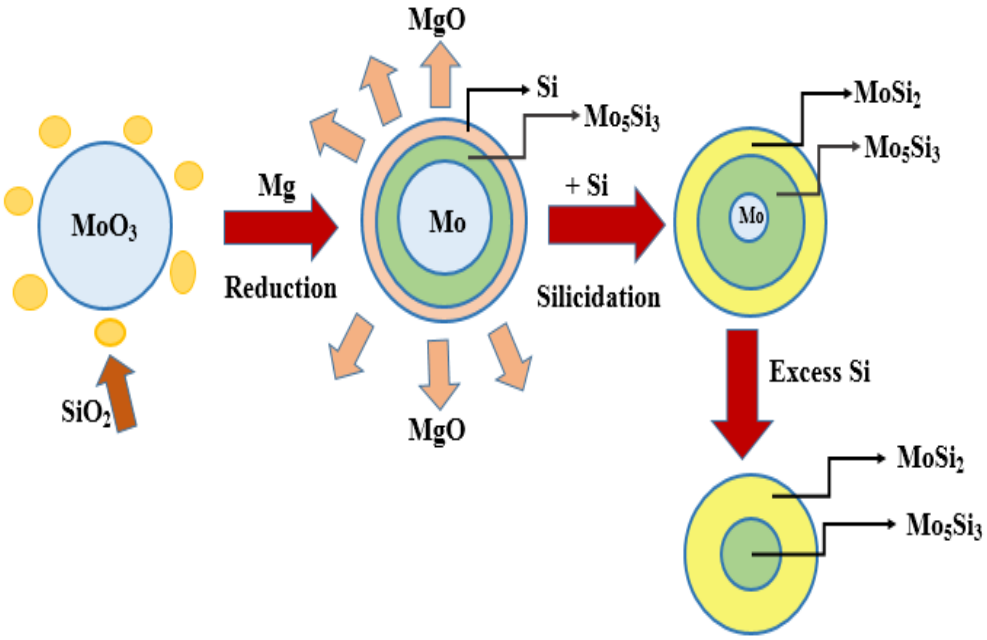

Fig 4.14 Schematic representation of transformation of MoO_3 to $MoSi_2$ nano-particles

4.4.2. Series II

The formation mechanism of molybdenum disilicide follows multistep process (i.e. reduction and silicidation) in an autoclave. In the present study MoO_3 acts as the molybdenum source, while as magnesium (Mg) and Si were used as reducing agent and silicon source, respectively. Along with Mg, silicon also reduced MoO_3 to Mo and molybdenum silicide products such as Mo_5Si_3 and $MoSi_2$.

The possible reaction paths given below shows the reduction of MoO_3 to Mo in an autoclave, when magnesium and silicon individually acted as reducing agents in MoO_3-Mg-Si system.

$$MoO_3 + 3Mg \rightarrow Mo + 3MgO \quad (4.15)$$

$$2MoO_3 + 3Si \rightarrow 2Mo + 3SiO_2 \quad (4.16)$$

Magnesium being highly reactive absorbs oxygen from autoclave to form MgO, which act as catalyst for the formation of $MoSi_2$ **[10]**. At different temperatures, heat of formation (ΔH) shows the nature of chemical reaction whether it requires heat or emits energy during the reaction. Among above reactions, more negative heat of formation (ΔH) has been calculated in reaction

(4.16) as shown in Fig 4.15, which depicted silicon as better reducing agent than magnesium in the opted system. Moreover, reduction of MoO_3 to Mo is also possible by the mixture of Mg and Si which is expressed as follows;

$$MoO_3 + Mg + Si \rightarrow Mo + SiO_2 + MgO \quad (4.17)$$

The value of ΔH of above reaction is more negative than reaction (4.15) but less negative than (4.16). This shows the higher feasibility of reaction (4.17) in the presence of Mg and Si than individual Mg in reaction (4.15). Among reaction (4.16) and (4.17), the reduction of MoO_3 to Mo is more feasible with silicon.

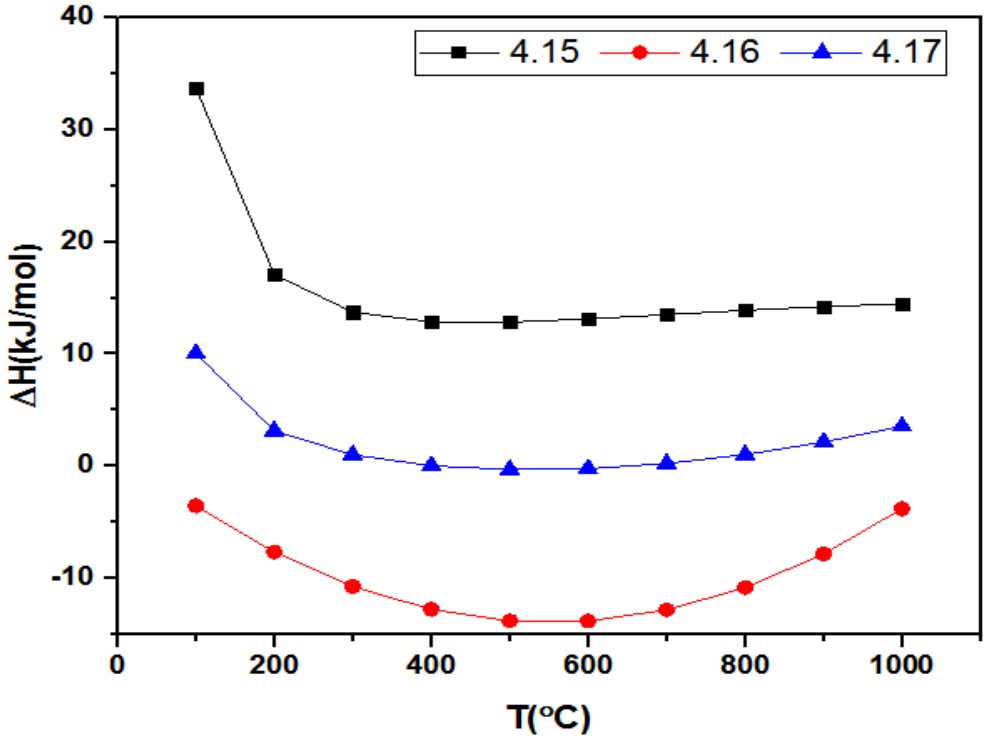

Fig. 4.15 Variation of ΔH at different temperature

Following reaction path ways have been framed for reduction-silicidation of MoO_3 in presence of Mg and Si in an autoclave.

$$5\ MoO_3 + 15\ Mg + 3Si \rightarrow Mo_5Si_3 + 15MgO \quad (4.18)$$

$$5\ MoO_3 + Mg + 3Si \rightarrow Mo_5Si_3 + MgO + 7SiO_2 \quad (4.19)$$

$$MoO_3 + 3Mg + Si \rightarrow MoSi_2 + 3MgO \quad (4.20)$$

$$MoO_3 + Mg + 3Si \rightarrow MoSi_2 + MgO + SiO_2 \quad (4.21)$$

$$6\ MoO_3 + 18\ Mg + 5Si \rightarrow MoSi_2 + Mo_5Si_3 + 18MgO \quad (4.22)$$

$$6\ MoO_3 + 2Mg + 13Si \rightarrow MoSi_2 + Mo_5Si_3 + 2MgO + 8SiO_2 \quad (4.23)$$

The ΔH variation of above reactions with temperature is shown in Fig 4.16. The reaction (4.23) shows the reduction of MoO_3 to Mo_5Si_3 with Mg and Si, which exhibits more negative ΔH variation than other reactions. However, with increase in temperature (above 600ºC) formation of molybdenum silicides (Mo_5Si_3 and $MoSi_2$) become more prominent than Mo_5Si_3 as observed in our XRD results also. This shows the accomplishment in reduction of MoO_3 to molybdenum silicides ($MoSi_2$ and Mo_5Si_3) with Mg and Si above 600ºC temperature.

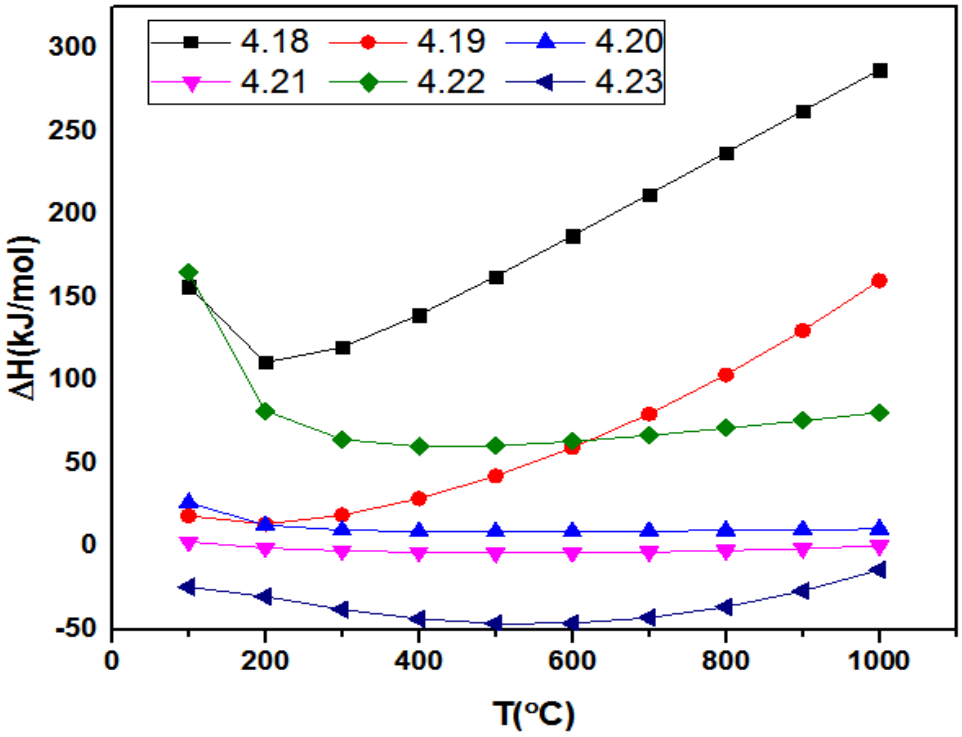

Fig. 4.16 Variation of ΔH at different temperature

This shows that the reduction –silicidation of MoO_3 to Mo, $MoSi_2$ and intermediate (Mo_5Si_3) takes place simultaneously **[1].**

The possible reaction path ways framed for the formation of molybdenum silicides from MoO3 and Mo, in presence of Mg and Si are shown below:

However, after the reduction of MoO_3 to Mo, in further stage the silicidation process might take place for the formation of Mo-Si compounds (Mo_5Si_3 and $MoSi_2$) which can be expressed by following chemical reactions;

$$5Mo + 3Si \rightarrow Mo_5Si_3 \quad (4.24)$$

$$Mo + 2Si \rightarrow MoSi_2 \quad (4.25)$$

$$6Mo + 5Si \rightarrow Mo_5Si_3 + MoSi_2 \quad (4.26)$$

The ΔH variation with temperature of above reactions is shown in Fig 4.17. The reaction (4.26) has more negative variation of ΔH with temperature, which shows the feasibility of the formation of molybdenum silicides such as Mo_5Si_3 and $MoSi_2$ as the reaction intermediates before pure phase $MoSi_2$ is formed.

$$Mo_5Si_3 + 7\ Si \rightarrow 5\ MoSi_2 \quad (4.27)$$

The reaction (4.27) possess more negative ΔH than reaction (4.26). The reaction between Si and as produced intermediate phased (Mo_5Si_3) results in the formation of silicon rich phase ($MoSi_2$) as shown in schematic representation (Fig 4.20, discussed later). Increase in temperature favors the formation of pure phase ($MoSi_2$).

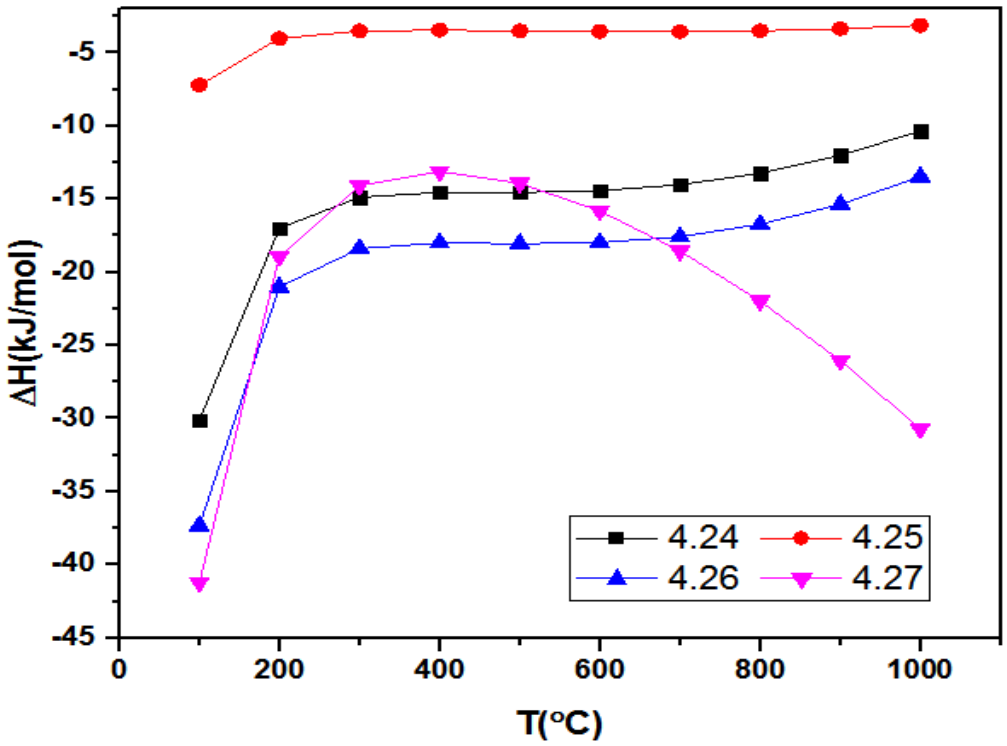

Fig 4.17 Variation of ΔH at different temperature

The possible reaction path ways framed for the formation of molybdenum silicides from MoO_3 and Mo, in the presence of Mg and Si in an autoclave is shown below:

$$2MoO_3 + Mo + 9Si \rightarrow 3MoSi_2 + 3SiO_2 \quad (4.28)$$

$$2MoO_3 + 3Mo + 6Si \rightarrow Mo_5Si_3 + 3SiO_2 \quad (4.29)$$

$$2MoO_3 + 4Mo + 8Si \rightarrow MoSi_2 + Mo_5Si_3 + 3SiO_2 \quad (4.30)$$

$$MoO_3 + Mo + 3Mg + 4Si \rightarrow 2\ MoSi_2 + 3MgO \quad (4.31)$$

$$MoO_3 + 4Mo + 3Mg + 3Si \rightarrow Mo_5Si_3 + 3MgO \quad (4.32)$$

$$MoO_3 + 5Mo + 3Mg + 5Si \rightarrow MoSi_2 + Mo_5Si_3 + 3MgO \quad (4.33)$$

The ΔH variation with temperature of above reactions is shown in Fig 4.18. The negative ΔH variation is given as follows:

(4.30 > 4.29 > 4.28 > 4.33 > 4.32 > 4.31)

Reaction (4.30) shows the most feasible reaction path formation of $MoSi_2$ and intermediate Mo_5Si_3. This shows both reduction of MoO_3 to Mo and Silicidation of Mo proceed simultaneously inside the autoclave.

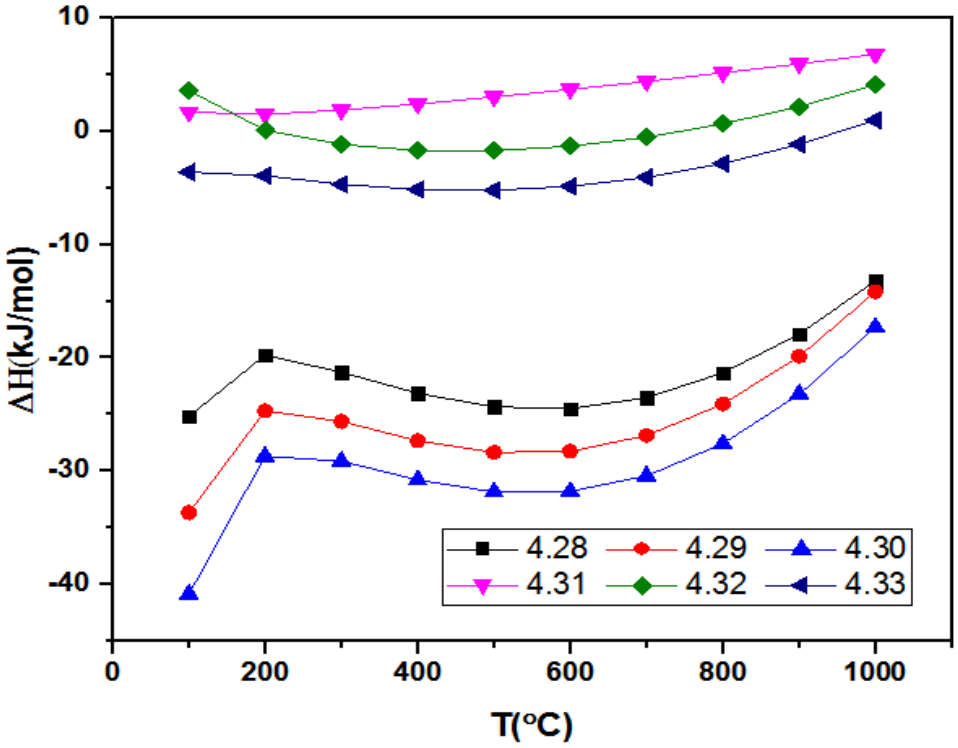

Fig 4.18 Variation of ΔH at different temperature

$$2MoO_3 + Mo + 5Si \rightarrow MoSi_2 + 3SiO_2 + Mo \quad (4.34)$$

$$2MoO_3 + 4Mo + 6Si \rightarrow Mo_5Si_3 + 3SiO_2 + Mo \quad (4.35)$$

$$2MoO_3 + 5Mo + 8Si \rightarrow MoSi_2 + Mo_5Si_3 + 3SiO_2 + Mo \quad (4.36)$$

$$MoO_3 + 2Mo + 3Mg + 4Si \rightarrow 2MoSi_2 + 3MgO + Mo \quad (4.37)$$

$$MoO_3 + 5Mo + 3Mg + 3Si \rightarrow Mo_5Si_3 + 3MgO + Mo \quad (4.38)$$

$$MoO_3 + 6Mo + 3Mg + 8Si \rightarrow MoSi_2 + Mo_5Si_3 + 3MgO + Mo \quad (4.39)$$

The following feasibility reaction path is followed in autoclave considering the ΔH variation with temperature as shown in Fig 4.19.

(4.35 > 4.36 > 4.34 > 4.39 > 4.38 > 4.37)

It shows that the reaction product molybdenum in first phase favors the formation of Mo-Si compounds (Mo_5Si_3 and $MoSi_2$). The variation of ΔH with temperature of reaction (4.35) is more negative than reaction (4.36). However, this trend of ΔH is followed up-to 650ºC. As the temperature is increased, the reaction (4.36) showed the more negative value of ΔH. Hence the reaction 4.36 is more feasible for formation of $MoSi_2$ and Mo_3Si_5. The formation mechanism has

been schematically represented in Fig 4.20. The decrease of Mo content with temperature and increase in silicide products shows that the reaction proceeds in forward direction with increase in temperature. The XRD results also predict the increase in phase formation with increase in temperature.

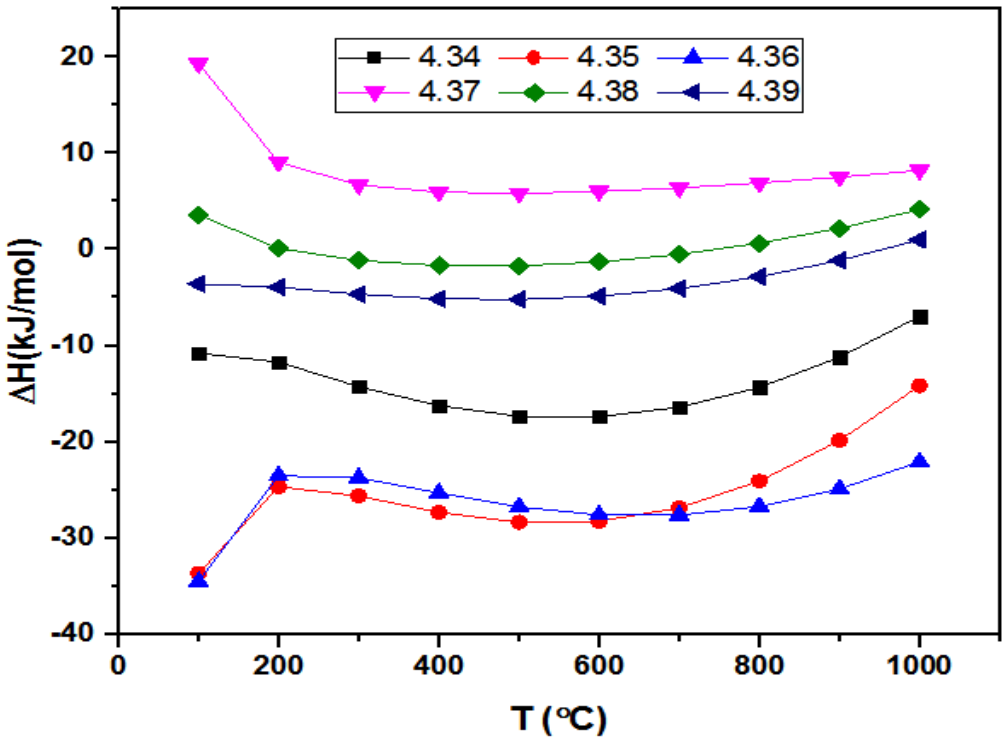

Fig 4.19 Variation of ΔH at different temperature

From above reaction, it can be concluded that MoO_3 is reduced to Mo with Mg and Si. Mo, Mo_5Si_3, $MoSi_2$, SiO_2 and MgO are the by-products formed after reduction. MgO is removed during leaching process. Further, the silicon reacted with Mo metal leading to the formation of silicide Mo_5Si_3 and $MoSi_2$ phase.

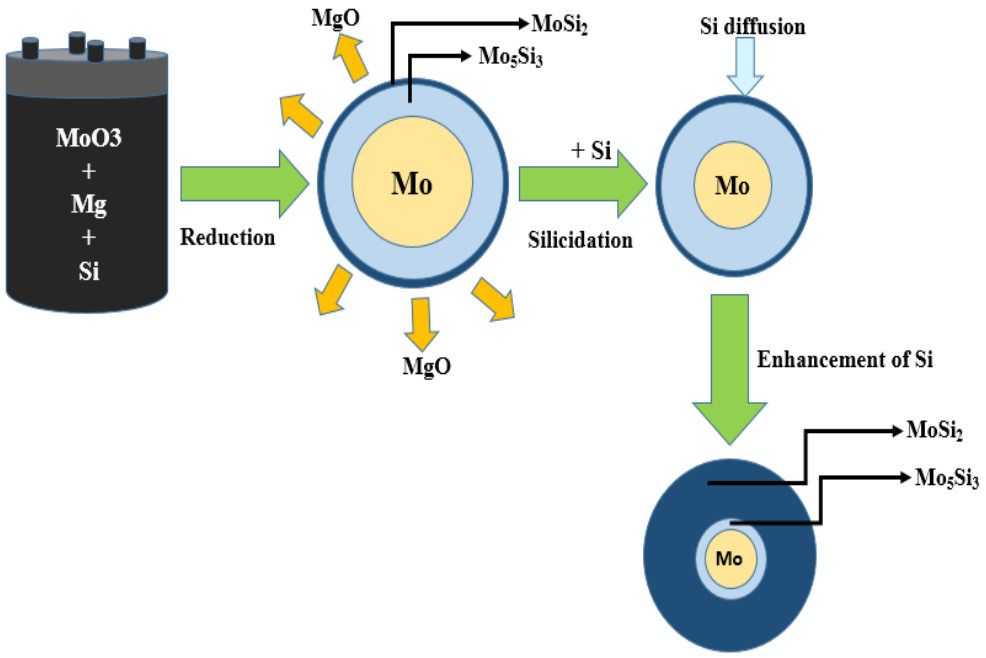

Fig 4.20 Schematic representation of transformation of MoO_3 to $MoSi_2$ nano-particles

References

[1] D. Ovali, D. Agaogullari, M.L. Ovecoglu, *Effects of excess reactant amounts on the mechano-chemically synthesized molybdenum silicides from MoO_3, SiO_2 and Mg blend,* International Journal of Refractory Metals and Hard Materials 65 (2016) 19-24.

[2] P. Feng. F. Akhtar, X. Du, H. Islam, *Effect of composition of starting materials of Mo-Si on the mechanically induced self- propagating reaction,* Journal of Alloys and Compounds 456 (2008) 304-307.

[3] M. Sannia, R. Orru, J.E. Garay, G. Cao, *Effect of phase transformation during high energy milling on field activated synthesis of dense $MoSi_2$,* Materials Science and Engineering A345 (2003) 270-277.

[4] R. Orru, J. Woolman, G. Cao, Z.A. Munir, *Advances in Sintering Science and Technology: Ceramics Transactions*, Journal of Materials Research 16 (2001) 1439.

[5] J. Xu, H. Zhang, J. Yan, B. Zhang, W. Li, *Effect of argon atmosphere on the formation of $MoSi_2$ by self- propagating combustion method,* International Journal of Refractory Metals and Hard Materials 25 (2007) 318-321.

[6] P. Kang, Z. Yin, *Phase formation during annealing as-milled powders of molybdenum disilicide*, Materials Letter 57 (2003) 4412-4417.

[7] B.K. Yen, T. Aizawa, J. Kihara, *Synthesis and formation mechanism of molybdenum silicides by mechanical alloying*, Materials Science and Engineering A220 (1996) 8-14.

[8] M. Ali, M. Liwa, *Modification of parameters in mechano-chemical synthesis to obtain <alpha> and <beta> molybdenum disilicide,* Advanced Powder Technology 24 (2013) 183-189.

[9] M. Zakeri, R.Y.Rad, M.H. Enayati, *Synthesis of nano-crystalline $MoSi_2$ by mechanical alloying*, Journal of Alloys and Compounds 403 (2005) 258-261.

[10] G. Singla, K. Singh, O.P. Pandey, *Structural and thermal analysis of in situ synthesized C–WC nano-composites*, Ceramics International 40 (2014) 5157–5164.

Conclusion

The synthesis of Molybdenum disilicide ($MoSi_2$) in an autoclave is systematically investigated. The effect of dwell time is investigated at 800 ºC and it is observed that increase in dwell time favors the formation of $MoSi_2$. Also, XRD results revealed that the formation of molybdenum disilicide enhanced with increase in the content of magnesium (Mg). The maximum content of $MoSi_2$ is obtained, when the Mg content is increased to 30% from stoichiometry ratio and heated at 900ºC for 10 hrs. In this case, $MoSi_2$ is obtained along with small traces of molybdenum (Mo) and molybdenum silicide (Mo_5Si_3) phase in dwell time 10hrs at 900ºC. The morphology of the best samples indicated that all the particles are agglomerated and exhibit irregular shape. Moreover, the spacing between the lattice fringes i.e. 0.22 nm obtained through HR-TEM matches with the plane (103) of $MoSi_2$ phase (ICDD 01-081-2167). Finally, it is concluded that, the molybdenum content must be decreased in order to obtain pure $MoSi_2$.

Future Scope

The present study provides detail understanding associated with the optimization of experimental procedure to obtain single phase $MoSi_2$ nano-powders. However, it is difficult to obtain $MoSi_2$ with the choice of starting reagent in stoichiometry ratio. So, the pure phase of $MoSi_2$ can be obtained through the present synthesis route by increasing the content of Mg and Si in starting reagent. Moreover, the oxidation resistance of $MoSi_2$ can be tested at various temperature to investigate the suitability of prepared sample at elevated temperatures. In addition, the electrical conductivity and corrosion resistance of the prepared sample can be performed.